Laser–Plasma Interaction Processes Observed in Direct-Drive-Implosion Experiments

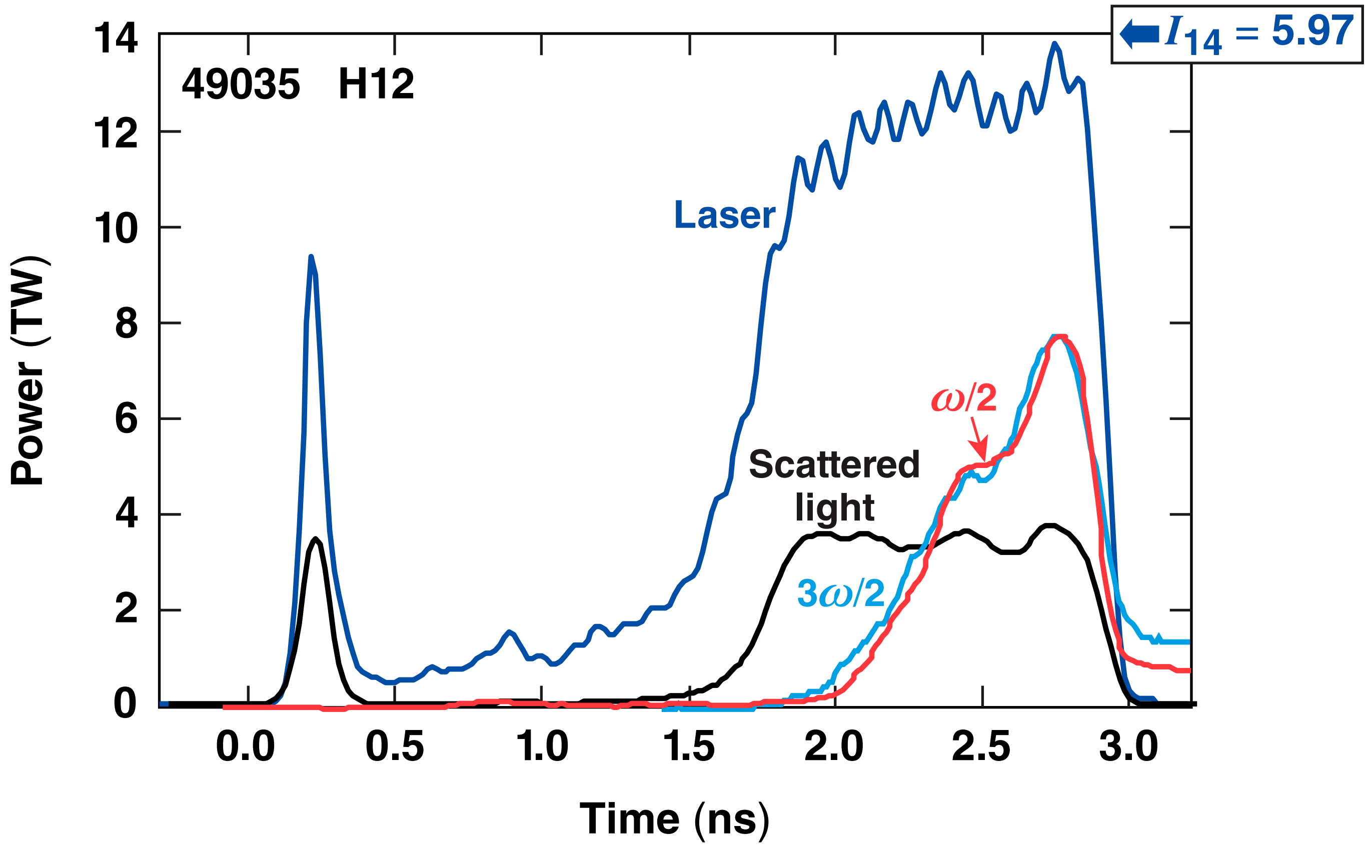

W. Seka *et al.*
University of Rochester
Laboratory for Laser Energetics

49th Annual Meeting of the
American Physical Society
Division of Plasma Physics
Orlando, FL
12–16 November 2007

Summary

Time-resolved scattered-light diagnostics provide unprecedented constraints for hydrodynamic simulations

- **Time-resolved absorption constrains the electron-heat transport in hydrodynamic simulations.**

  → **nonlocal electron-transport model* in *LILAC***

- **The coronal evolution is recorded in the overall scattered-light spectrum and further constrains heat transport.**
- **Laser–plasma interaction processes are identified through their spectral signatures.**
  - **enhanced scattering (cross-beam energy transfer)**
  - **two-plasmon-decay instability**
- **High-Z doping of plastic shells reduces energetic electron production due to two-plasmon-decay instability.**

E16201

*V. N. Goncharov (GI1.00001)

Collaborators

D. H. Edgell, J. P. Knauer, C. Stoeckl, V. N. Goncharov, J. A. Delettrez,
I. V. Igumenshchev, J. Myatt, A. V. Maximov, R. W. Short, and T. C. Sangster

University of Rochester
Laboratory for Laser Energetics

D. Shvarts

Nuclear Research Center
Negev, Israel

Outline

- Time-resolved absorption measurements
- Overall scattered-light spectrum near λ_L
  → coronal plasma evolution → electron-heat transport
- Enhanced absorption at early times
  → critical for first shock in implosion experiments
- Decreased absorption due to cross-beam energy transfer during the main pulse
- Two-plasmon-decay instability
  → fast-electron preheat

Time-Resolved Absorption

Time-resolved absorption is inferred from scattered-light measurements

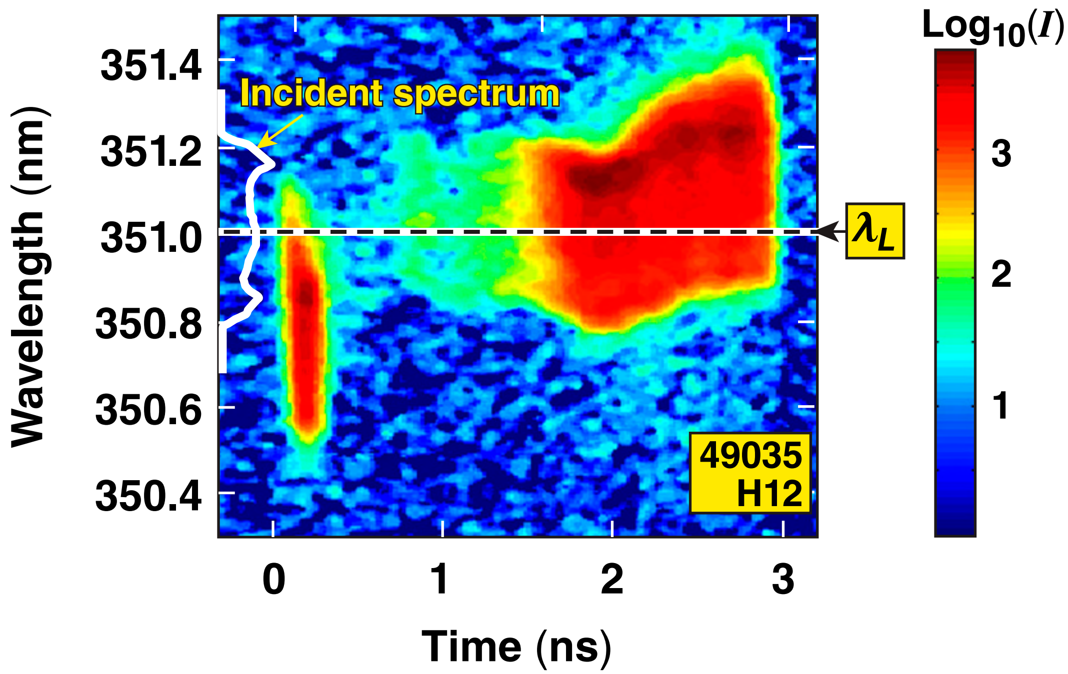

- Isotropic scattering is assumed (supported by simulations).
- Scattered light is measured with calorimeters behind and between focusing lenses.
- Time-resolved spectroscopy of scattered laser light provides detailed information on interaction processes.
- Scattered light power ($r = 1 - \alpha$) will be compared to simulations

E16203

Time-resolved scattered-light measurements require reexamination of electron-heat transport in simulations

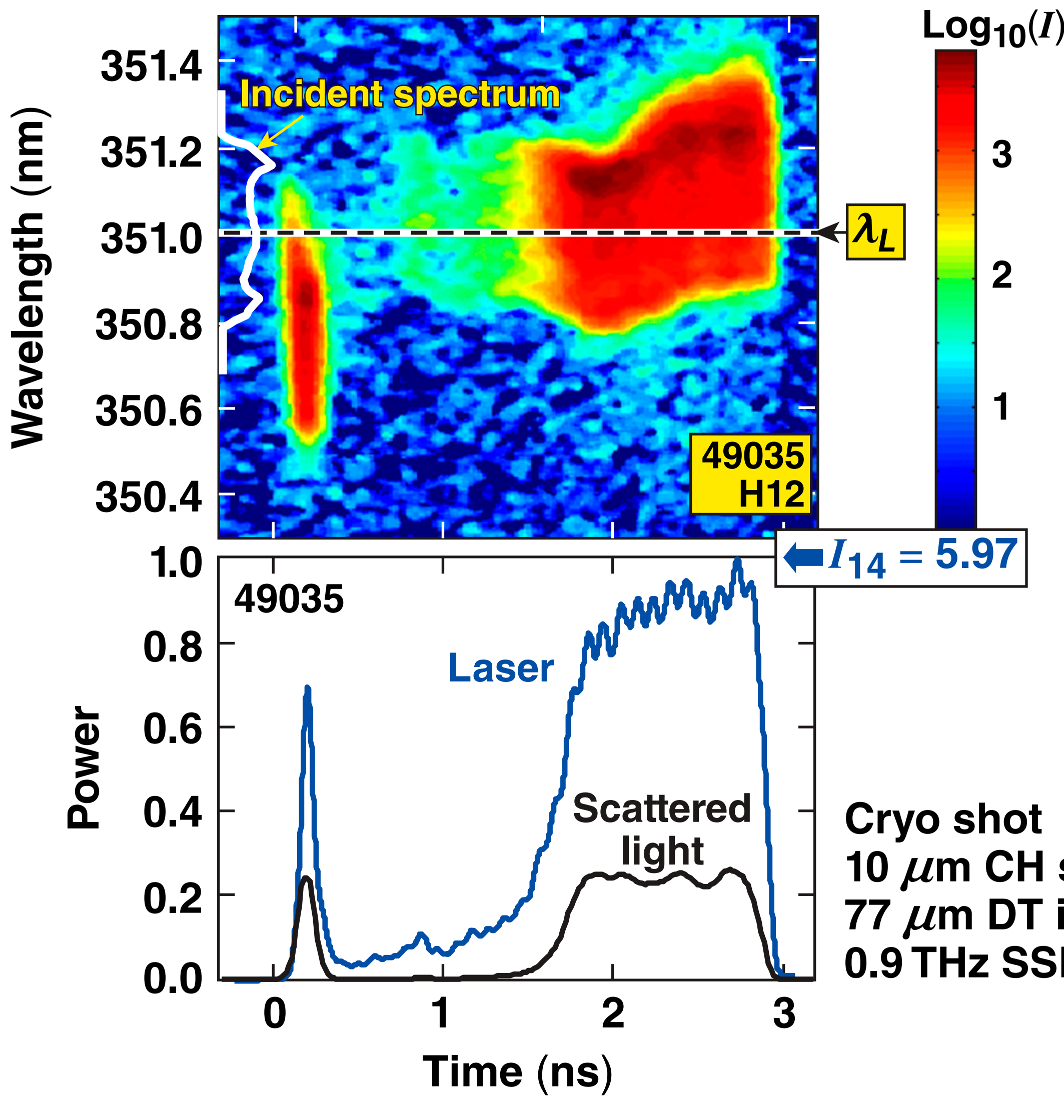

Cryo shot
10 μm CH shell
77 μm DT ice
0.9 THz SSD

E16203a

Time-resolved scattered-light measurements require reexamination of electron-heat transport in simulations

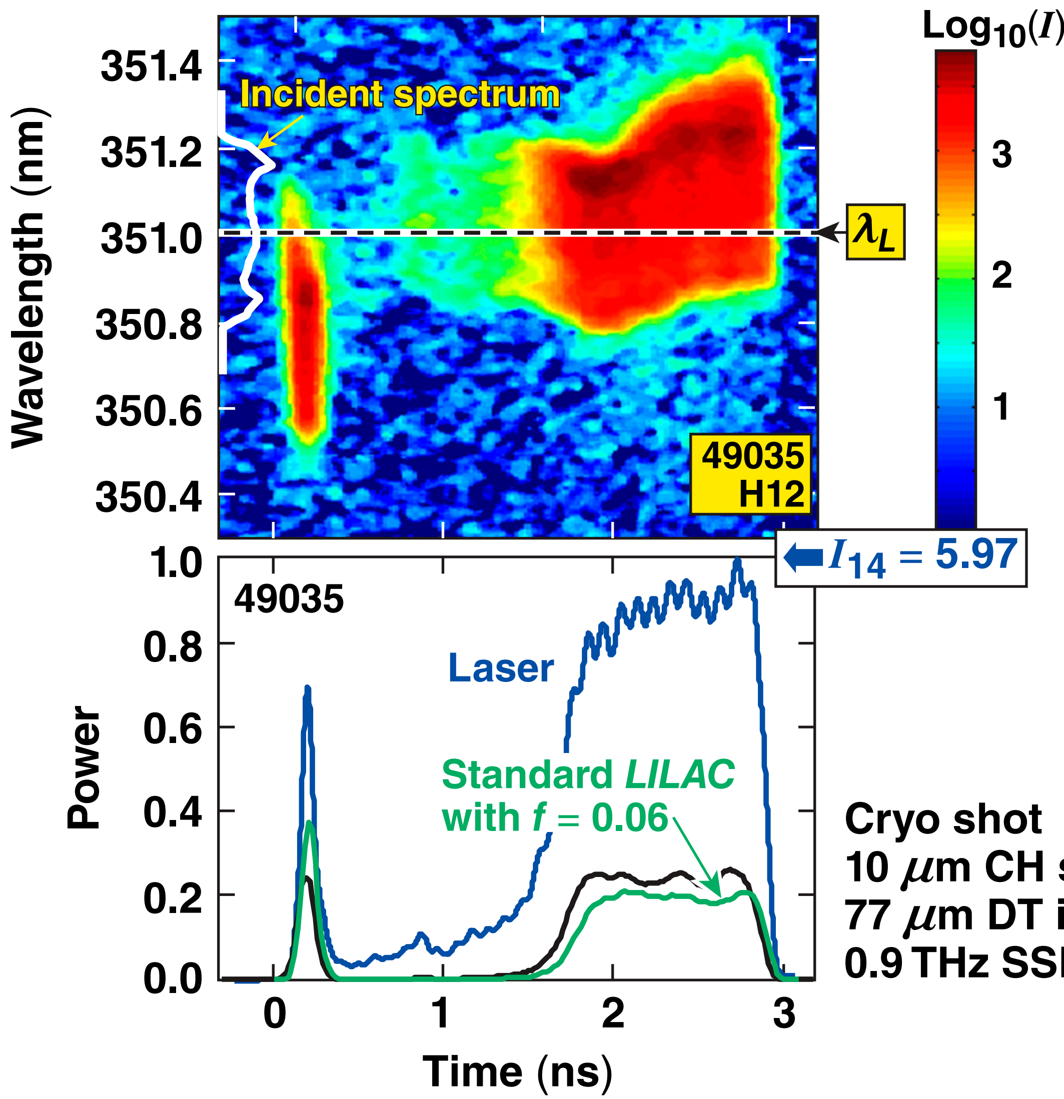

Cryo shot
10 μm CH shell
77 μm DT ice
0.9 THz SSD

E16203b

Time-resolved scattered-light measurements require reexamination of electron-heat transport in simulations

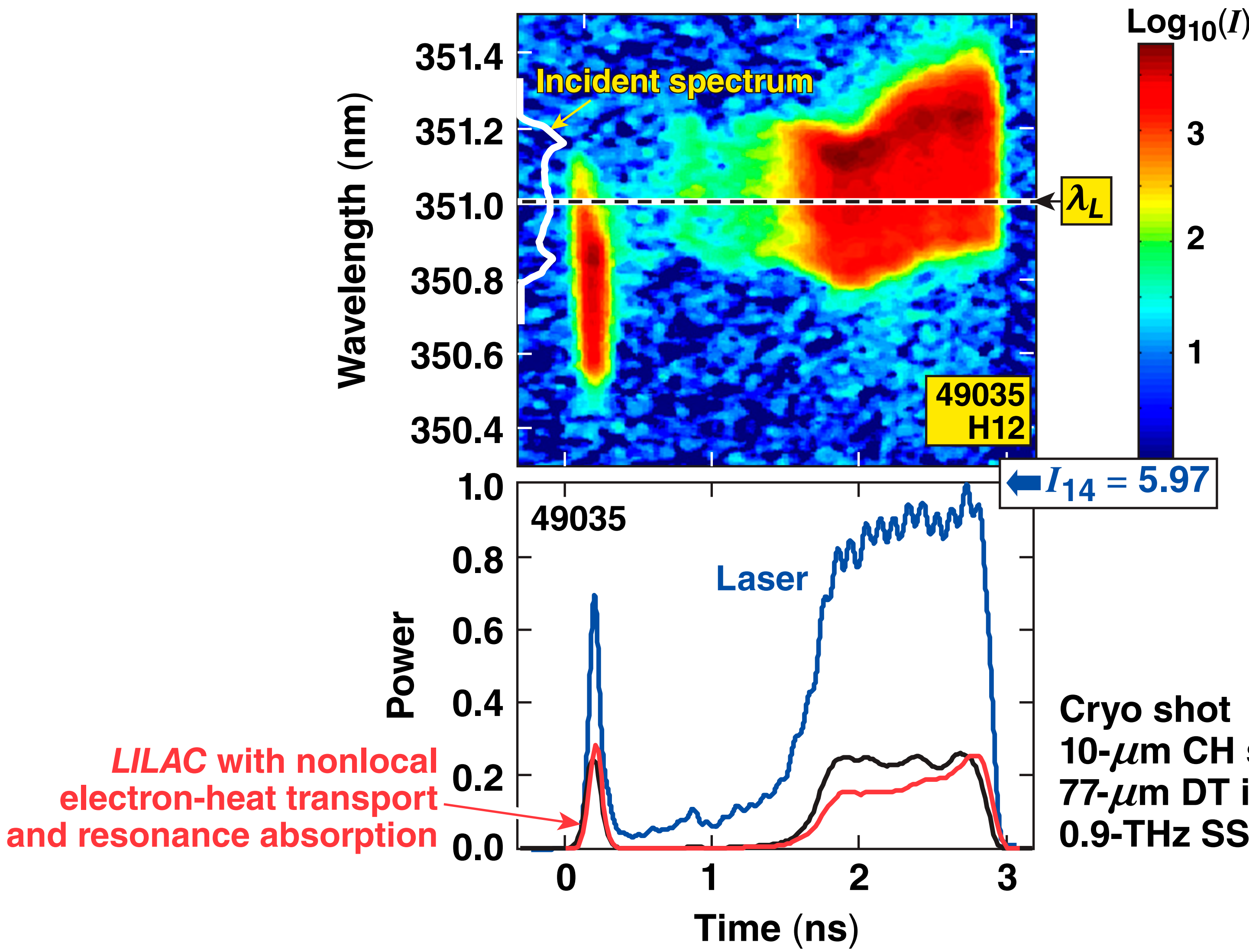

Cryo shot
10-μm CH shell
77-μm DT ice
0.9-THz SSD

E16203c

Time-resolved scattered-light measurements require reexamination of electron-heat transport in simulations

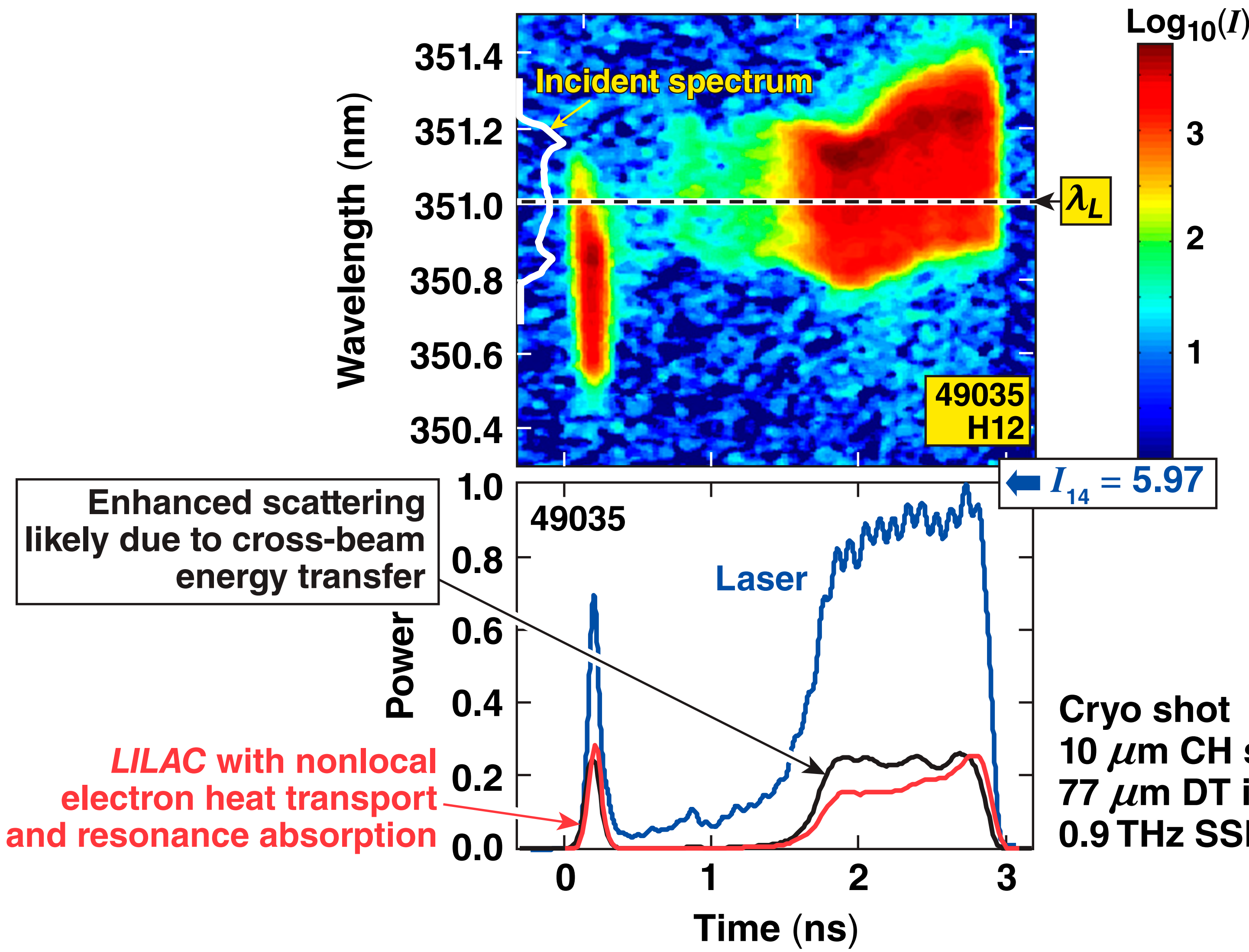

Cryo shot
10 μm CH shell
77 μm DT ice
0.9 THz SSD

E16203d

The frequency shift is proportional to the rate of change of the optical path

$$\Delta\omega \propto -\frac{\partial}{\partial t}\int \mu ds,\ \mu = \sqrt{1 - n_e/n_c}$$

→ an increasing path length through the plasma causes a blue shift in the spectrum

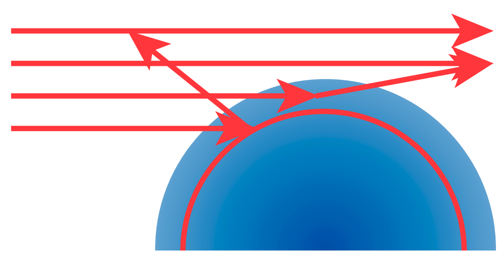

for details, see D. H. Edgell NO6.00009

The frequency shift is proportional to the rate of change of the optical path

$$\Delta\omega \propto -\frac{\partial}{\partial t}\int \mu \mathrm{d}s,\ \mu = \sqrt{1-n_e/n_c}$$

→ an increasing path length through the plasma causes a blue shift in the spectrum

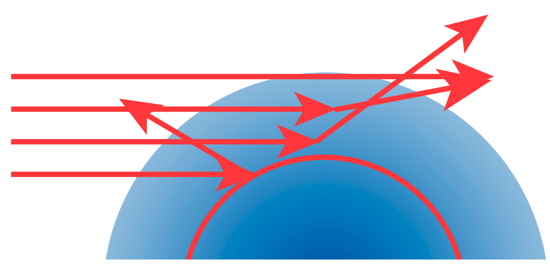

E16204a

for details, see D. H. Edgell NO6.00009

The frequency shift is proportional to the rate of change of the optical path

$$\Delta\omega \propto -\frac{\partial}{\partial t}\int \mu ds, \; \mu = \sqrt{1 - n_e/n_c}$$

→ an increasing path length through the plasma causes a blue shift in the spectrum

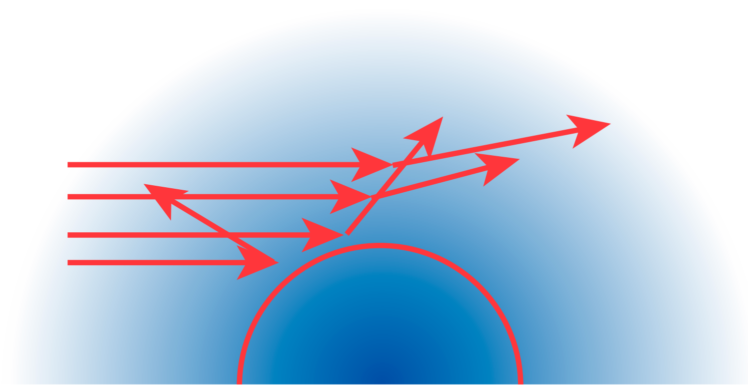

E16204b

for details, see D. H. Edgell NO6.00009

The scattered-light spectrum near λ_L is affected by the temporally changing optical-path length inside the corona

$$\Delta\omega \propto -\frac{\partial}{\partial t}\int \mu ds,\ \mu = \sqrt{1 - n_e/n_c}$$

→ an increasing path length through the plasma causes a blue shift in the spectrum

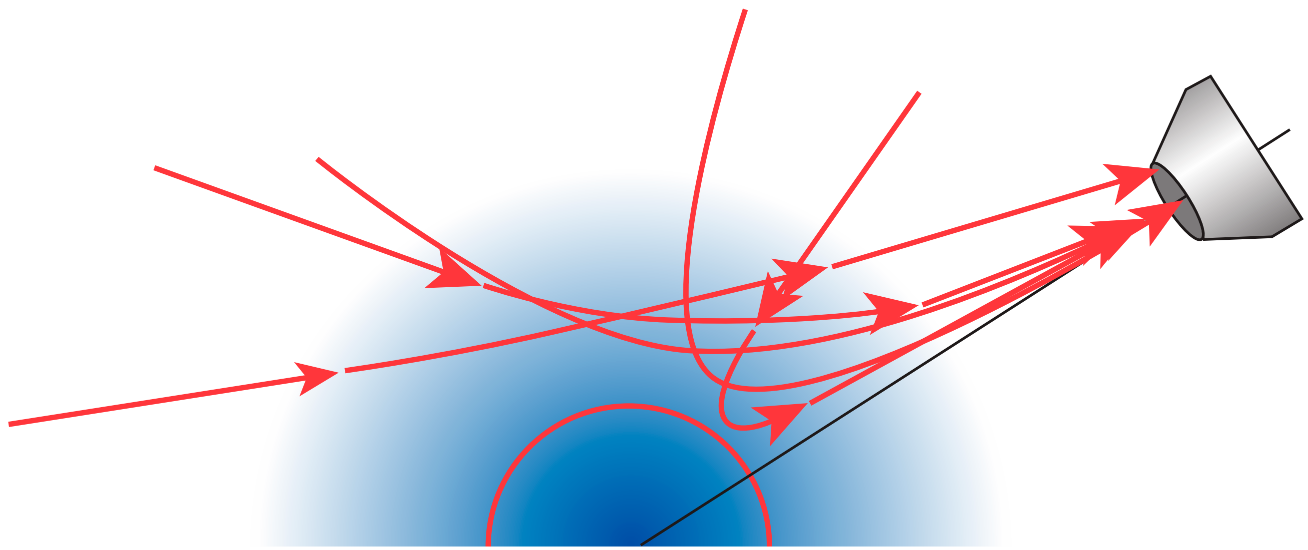

- All 60 beams of OMEGA contribute to the scattered-light signal seen by the camera
- The intensity and spectrum due to each beam varies with time and location of the beam relative to the camera

Including nonlocal thermal transport in *LILAC* reproduces the observed spectrum quite well

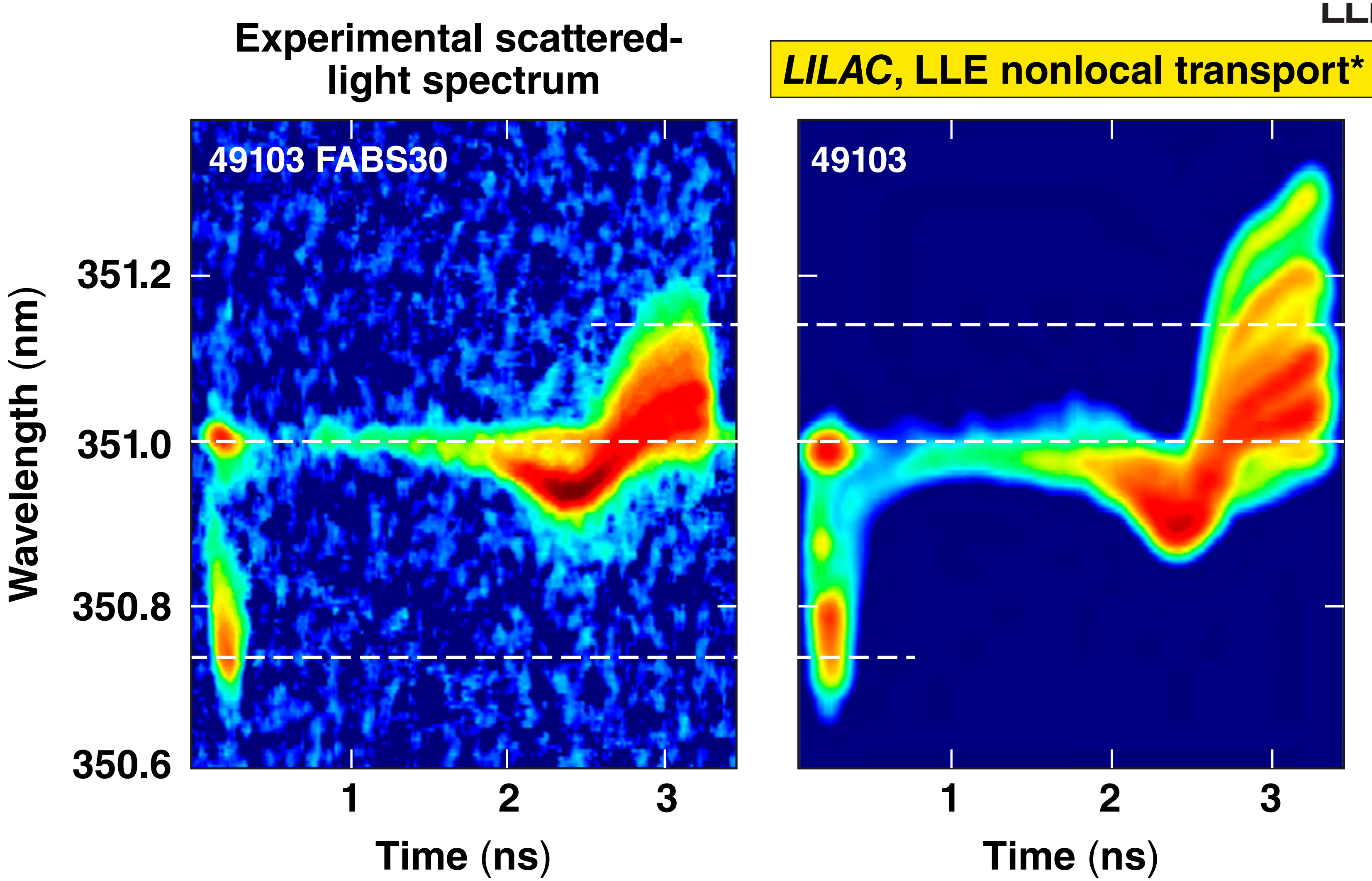

Cryo shot, 10 μm CD shell, 95 μm D_2 ice, no SSD

E16205

*V. N. Goncharov (GI1.00001), D. H. Edgell (NO6.00009)

Simulating the scattered-light spectrum requires fine-tuning of electron-heat transport

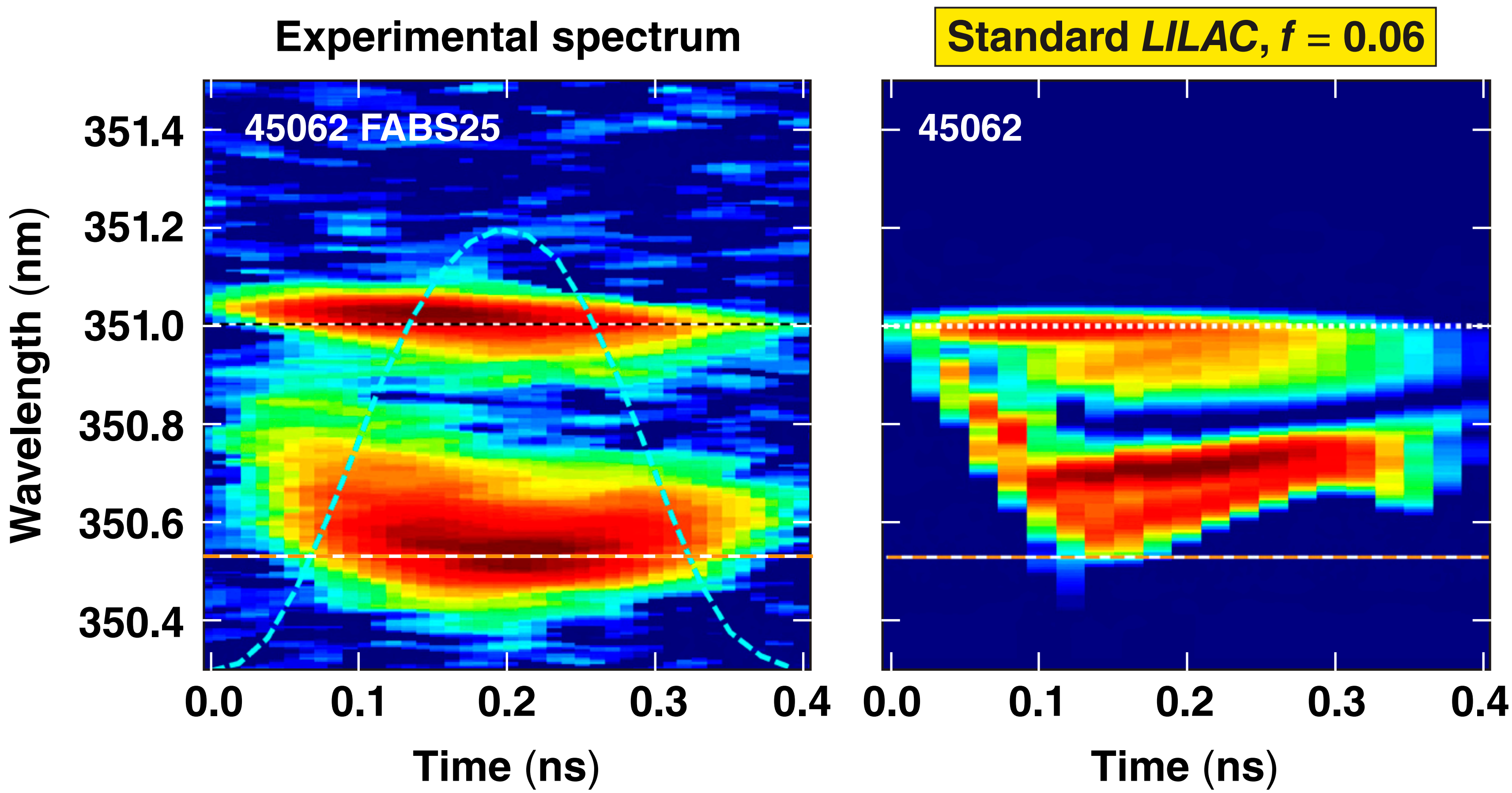

E16311

Simulating the scattered-light spectrum requires fine-tuning of electron-heat transport

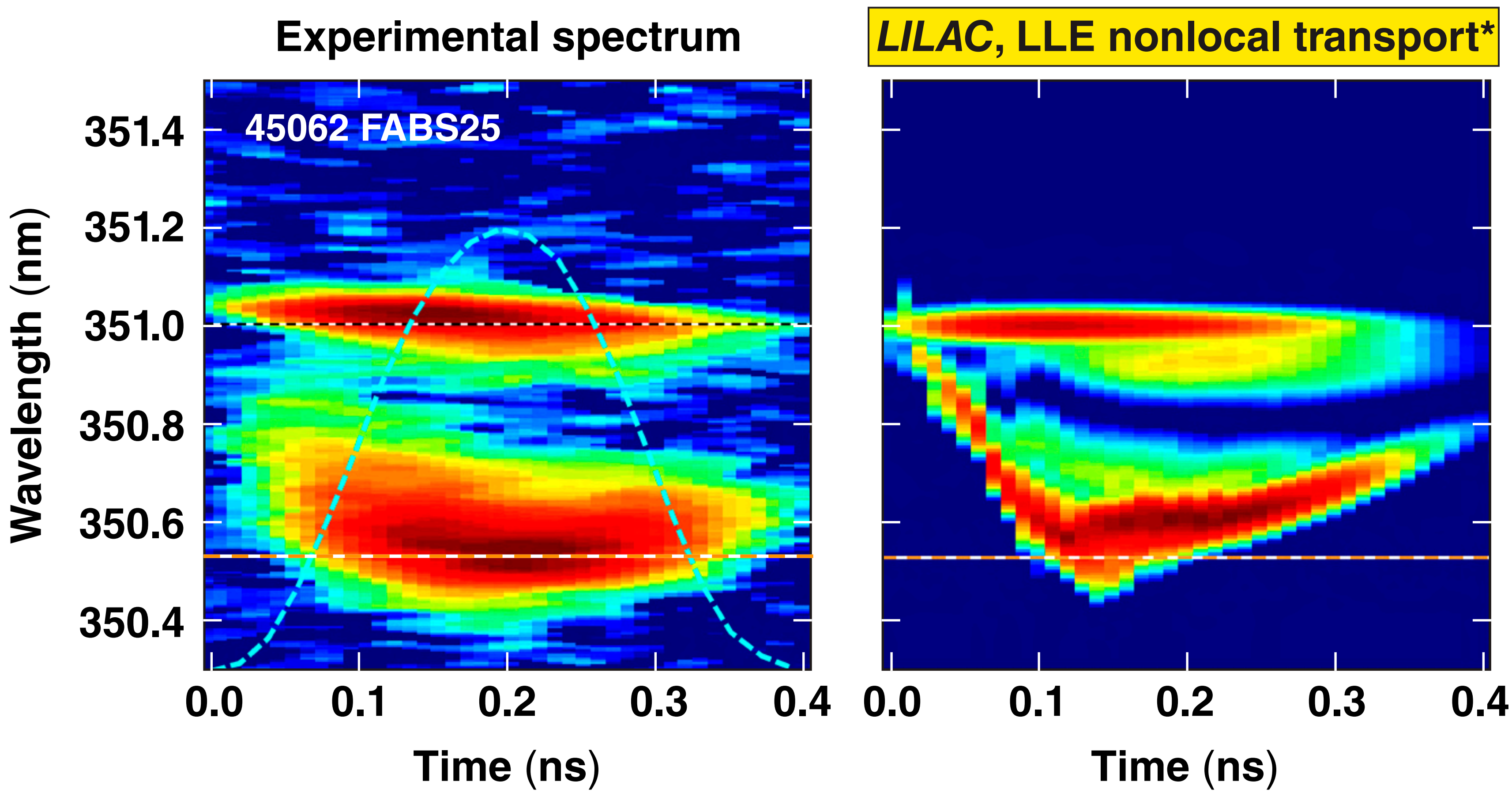

E16311b

*V. N. Goncharov (GI1.00001)

Nonlocal transport is required to model absorption during the first 100 to 200 ps

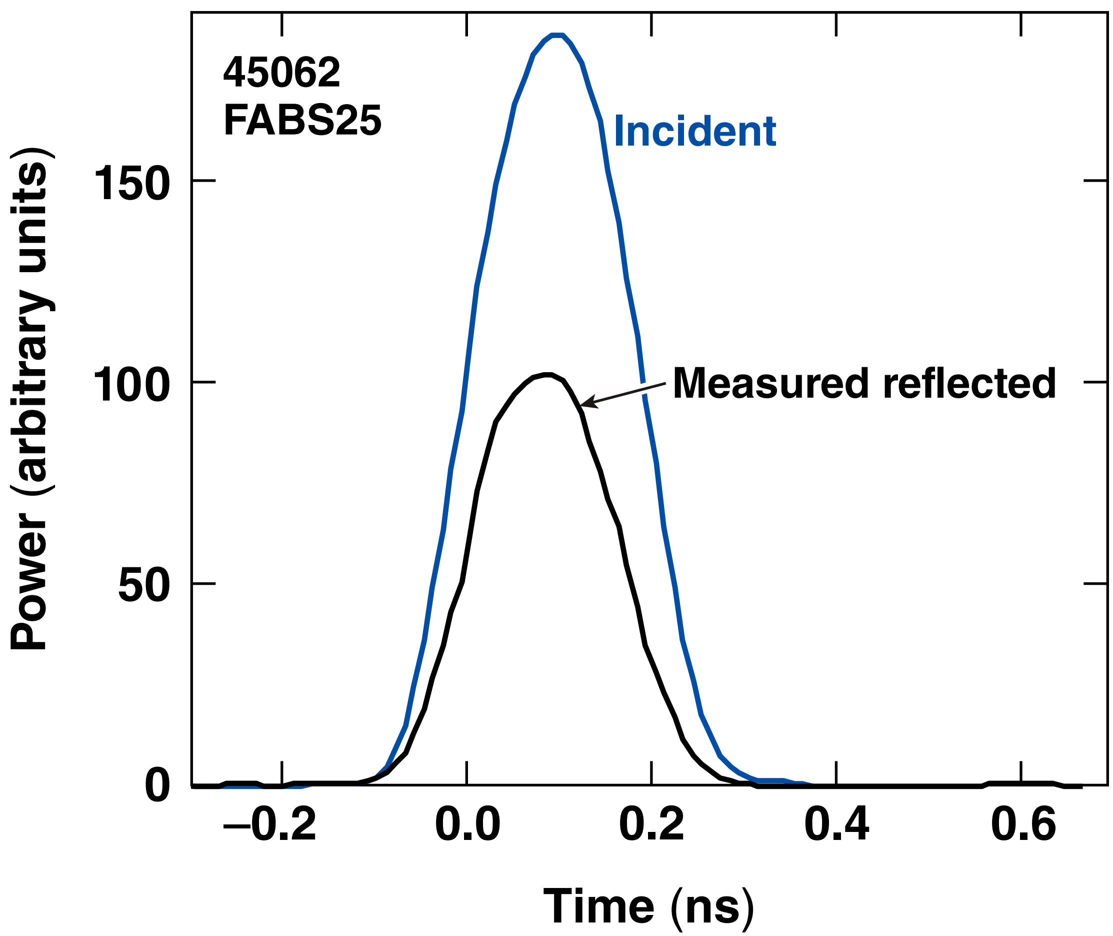

Warm 20 μm CH shell
60 beams
no SSD

E16206

Nonlocal transport is required to model absorption during the first 100 to 200 ps

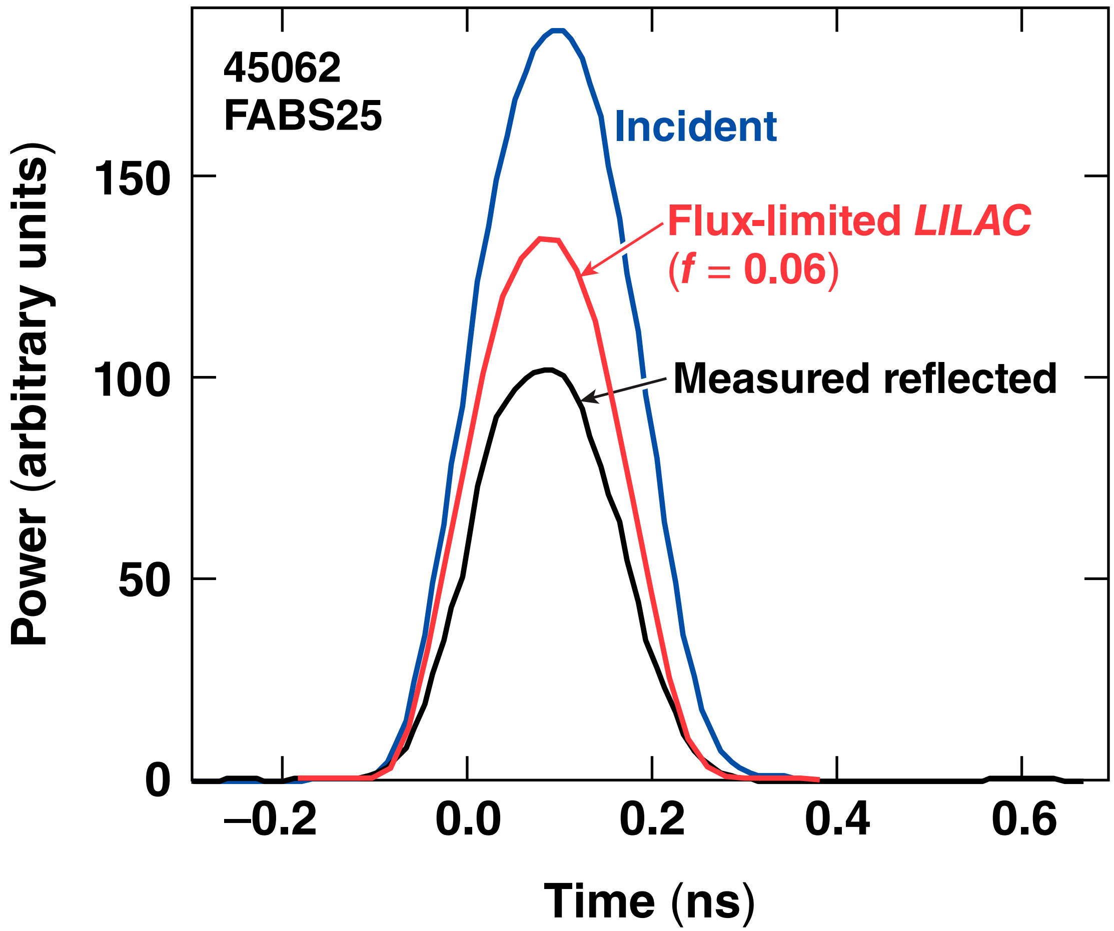

Warm 20 μm CH shell
60 beams
no SSD

E16206a

Nonlocal transport is required to model absorption during the first 100 to 200 ps

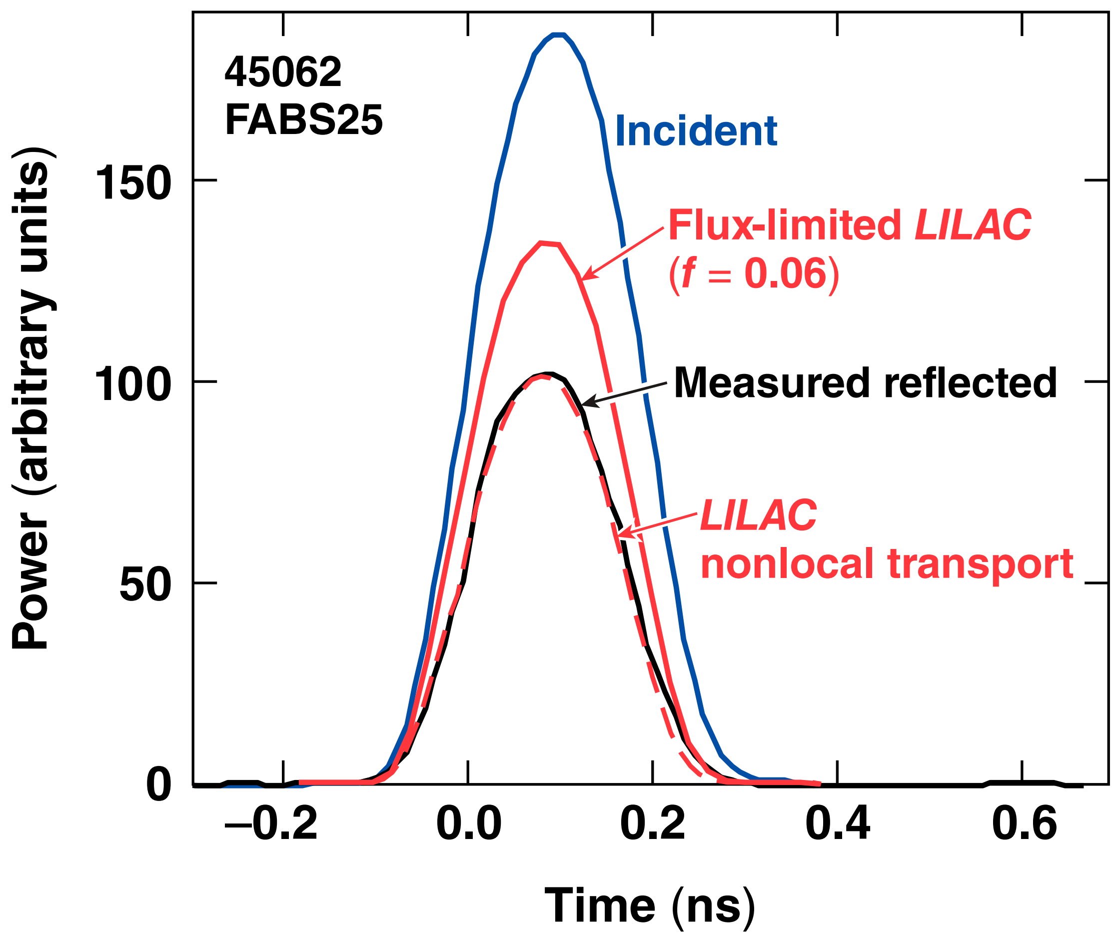

Warm 20 μm CH shell
60 beams
no SSD

E16206b

LILAC with nonlocal transport reproduces experimental absorption at early times

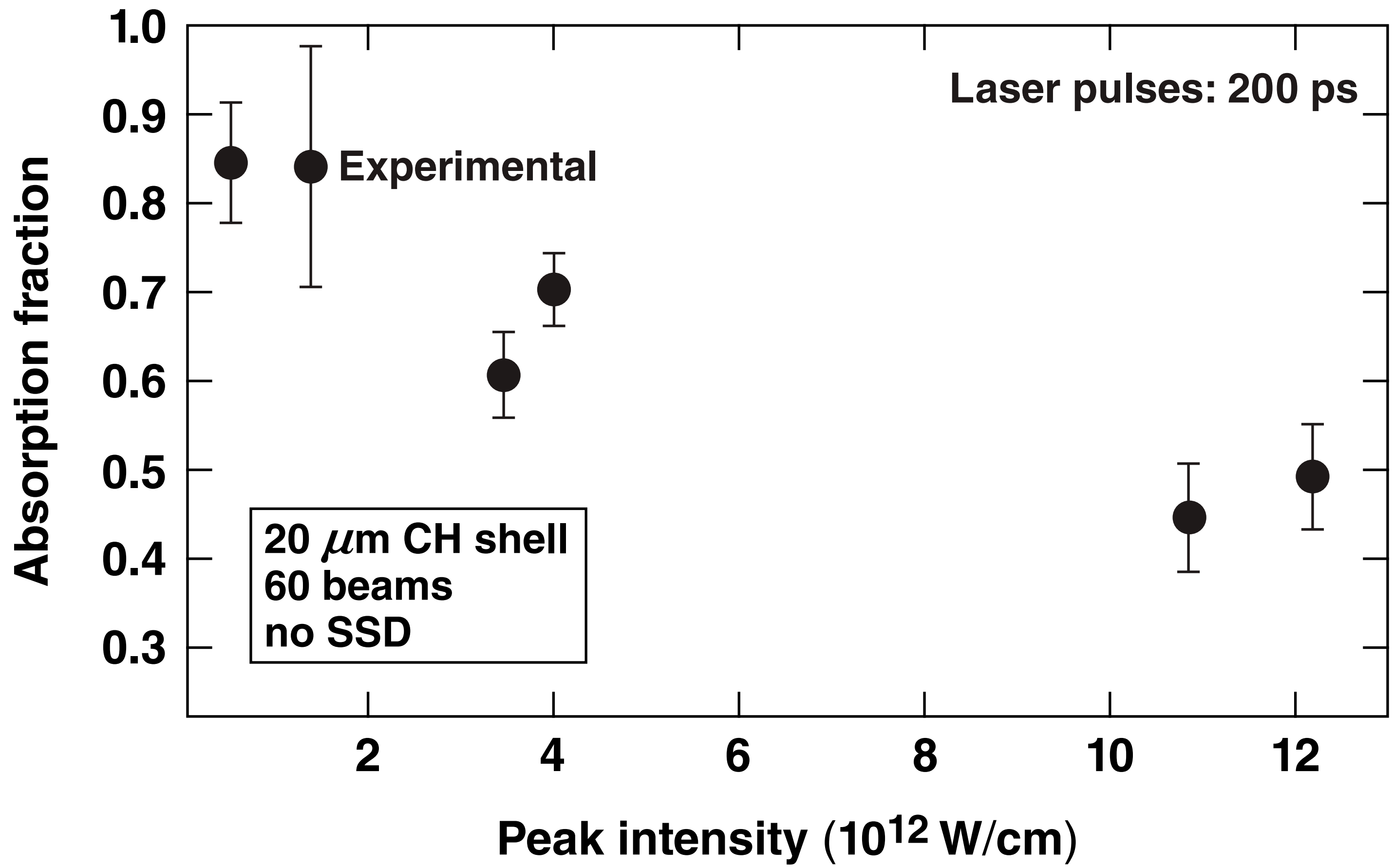

E16207

LILAC with nonlocal transport reproduces experimental absorption at early times

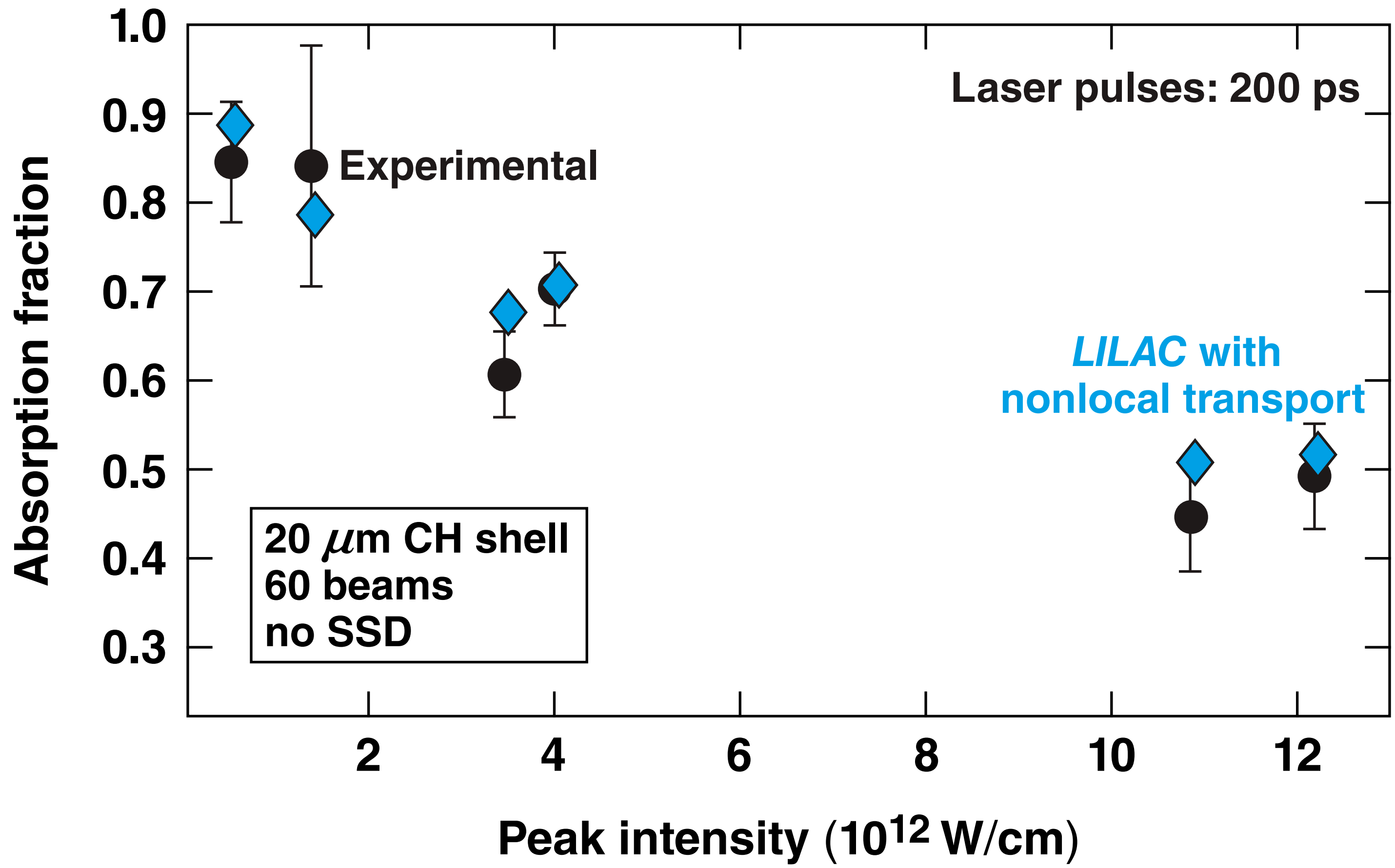

Precise modeling of initial absorption is essential for setting up low-adiabat-implosion experiments.

E16207a

Enhanced scattering at later times is consistent with SBS cross-beam energy transfer

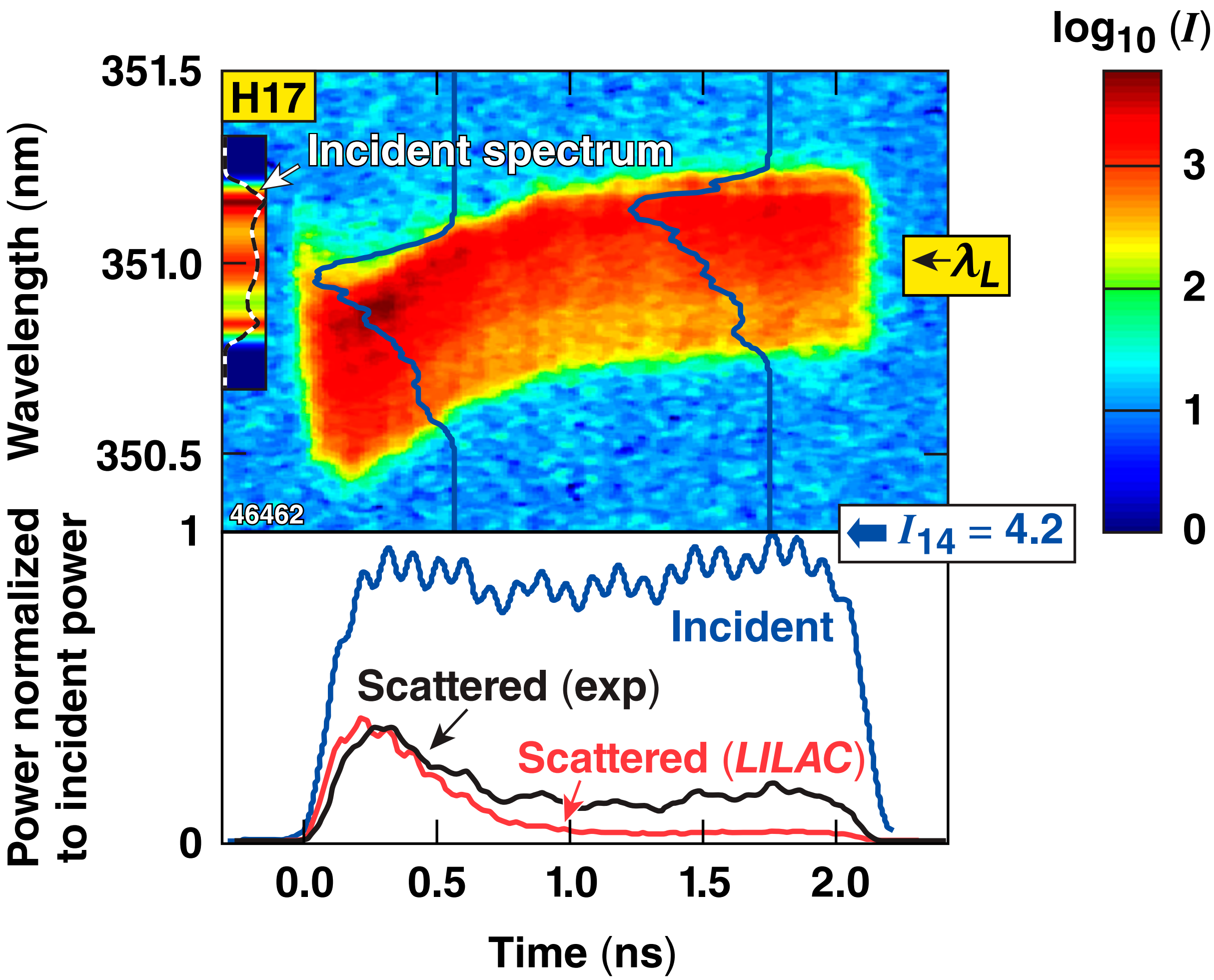

- Scattered-light spectrum is almost always red-peaked
  - nonlinear process must be involved

Enhanced scattering at later times is consistent with SBS cross-beam energy transfer

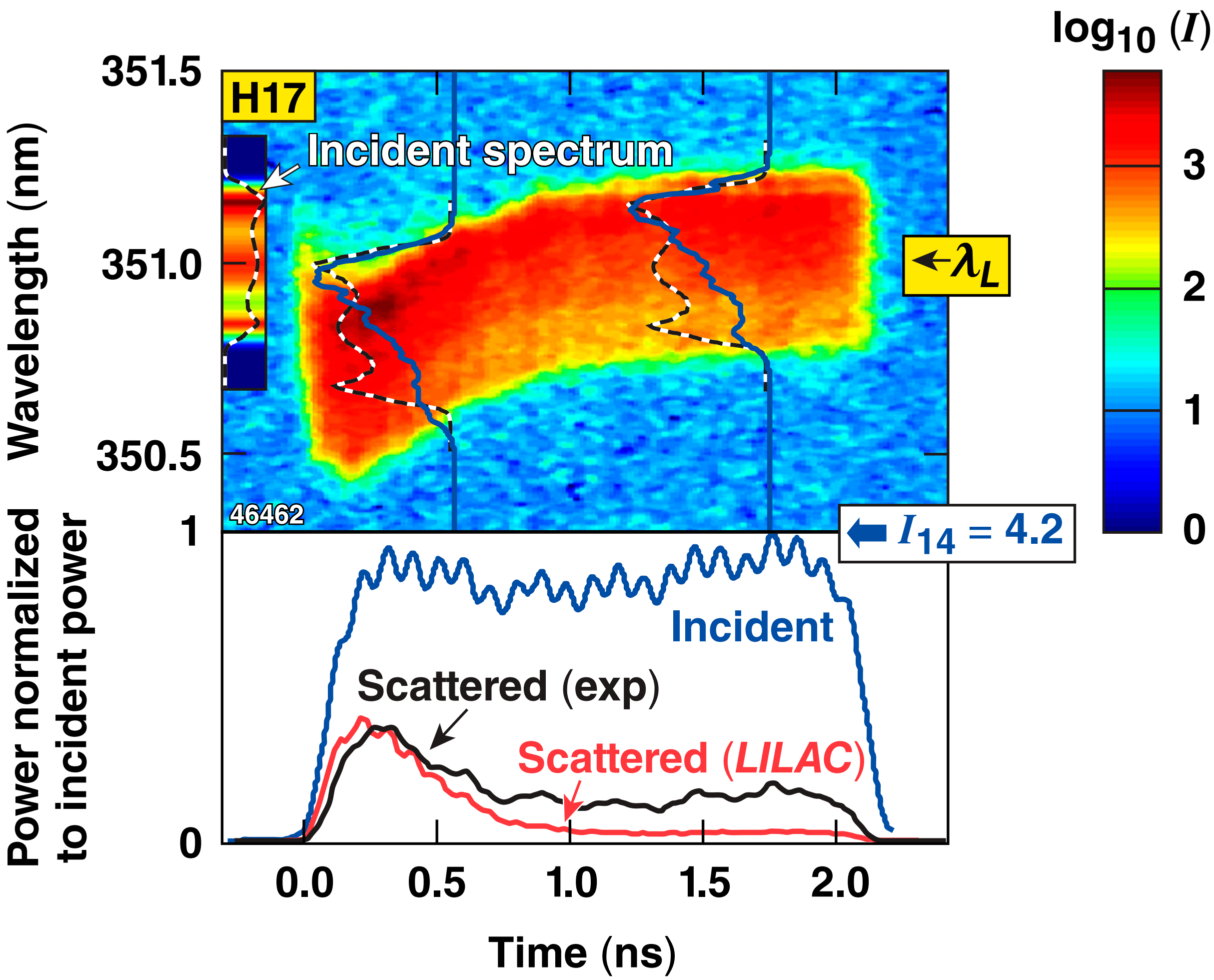

- Scattered-light spectrum is almost always red-peaked
  - nonlinear process must be involved

E16208a

Enhanced scattering at later times is consistent with SBS cross-beam energy transfer

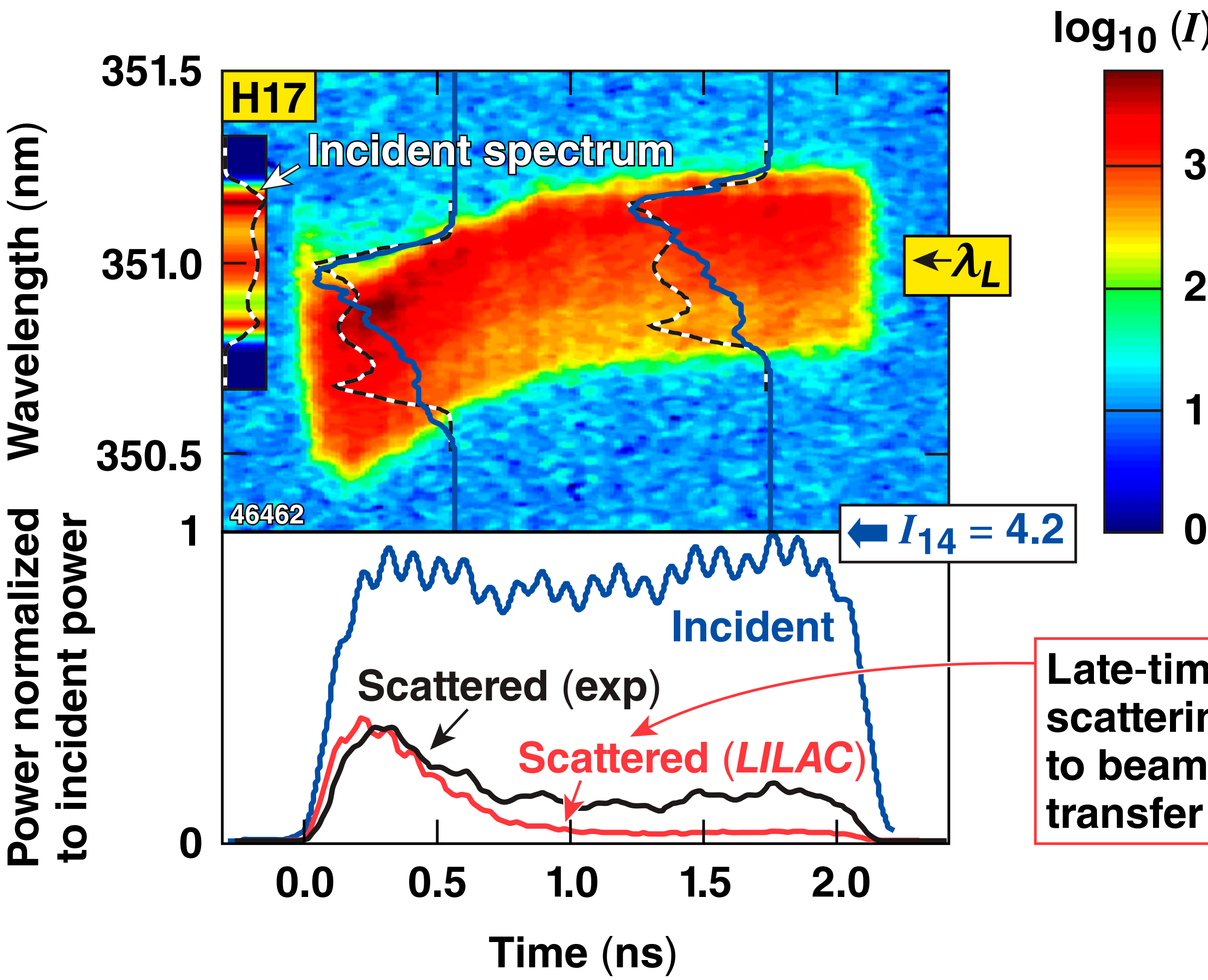

- Scattered-light spectrum is almost always red-peaked
  – nonlinear process must be involved

Late-time increased scattering likely to be due to beam-to-beam energy transfer via EM-seeded SBS.

Enhanced Scattering

Cross-beam energy transfer has been observed in OMEGA EM-seeded SBS experiments* as well as in LLNL** experiments

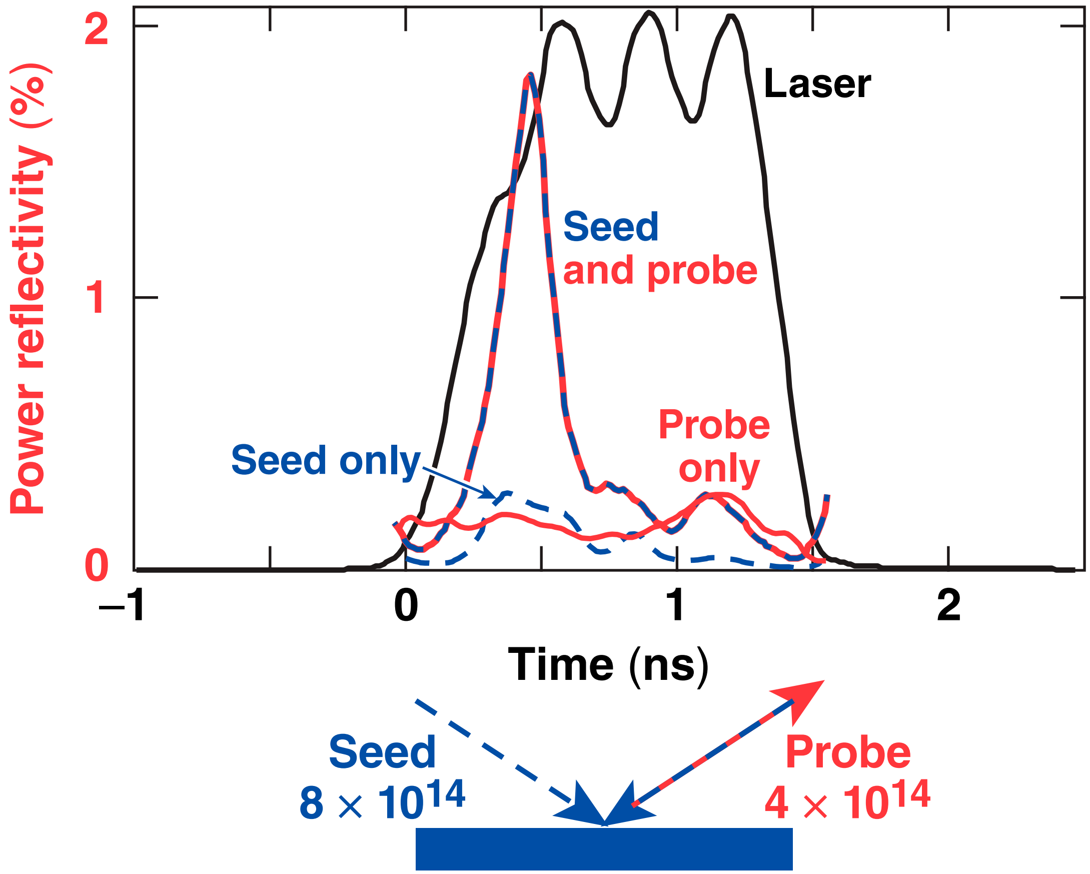

Enhanced scattering more modestly affects the second shock in implosion experiments with complex pulse shapes.

E16209

* W. Seka *et al*., Phys. Rev. Lett. 89 175002 (2002).

** R. K. Kirkwood, Phys. Rev. Lett. 89 215003 (2002).

The two-plasmon-decay (TPD) instability is observed in direct-drive spherical implosion experiments

Characteristics of this instability

- Decay of an incident photon into two plasmons near $n_c/4$
- Low-intensity threshold
  - for plane waves in linear density gradient*

    $\eta_{th} \sim I_{14} \, L_n / 230\, T_e$ (threshold parameter)**
- Energetic electron production
- Practical theories applicable to real experimental conditions are not presently available.
- TPD instability is identifiable in $3\omega/2$, $\omega/2$, and hard-x-ray spectra

E16211

* A. Simon *et al*., Phys. Fluids 26, 3107 (1983).
** J. A. Delettrez, JO3.00003

$3\omega/2$ and $\omega/2$ emission are indicative of the two-plasmon-decay instability and concomitant fast-electron generation

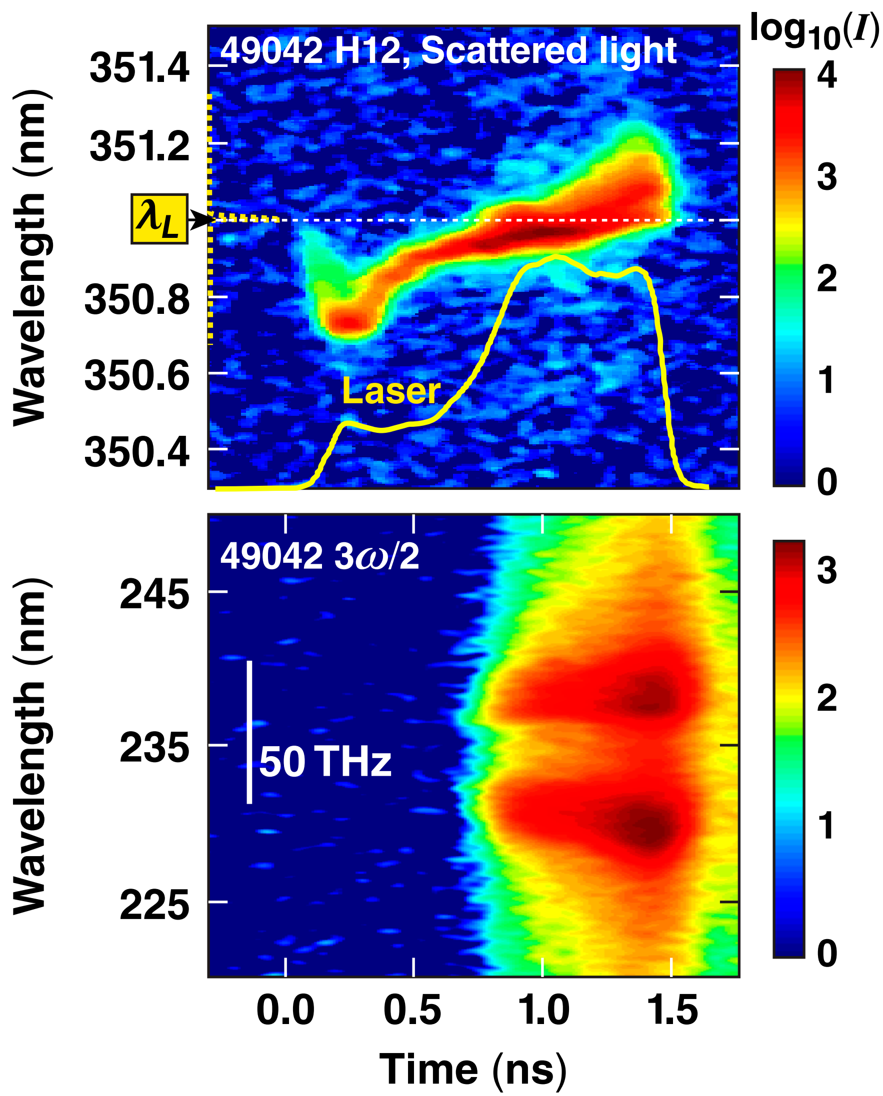

Warm 10 μm Si(6%)CH + 14 μm CD shell, 849-μm diam, 60 beams, No SSD

E16309

3ω/2 and ω/2 emission are indicative of the two-plasmon-decay instability and concomitant fast-electron generation

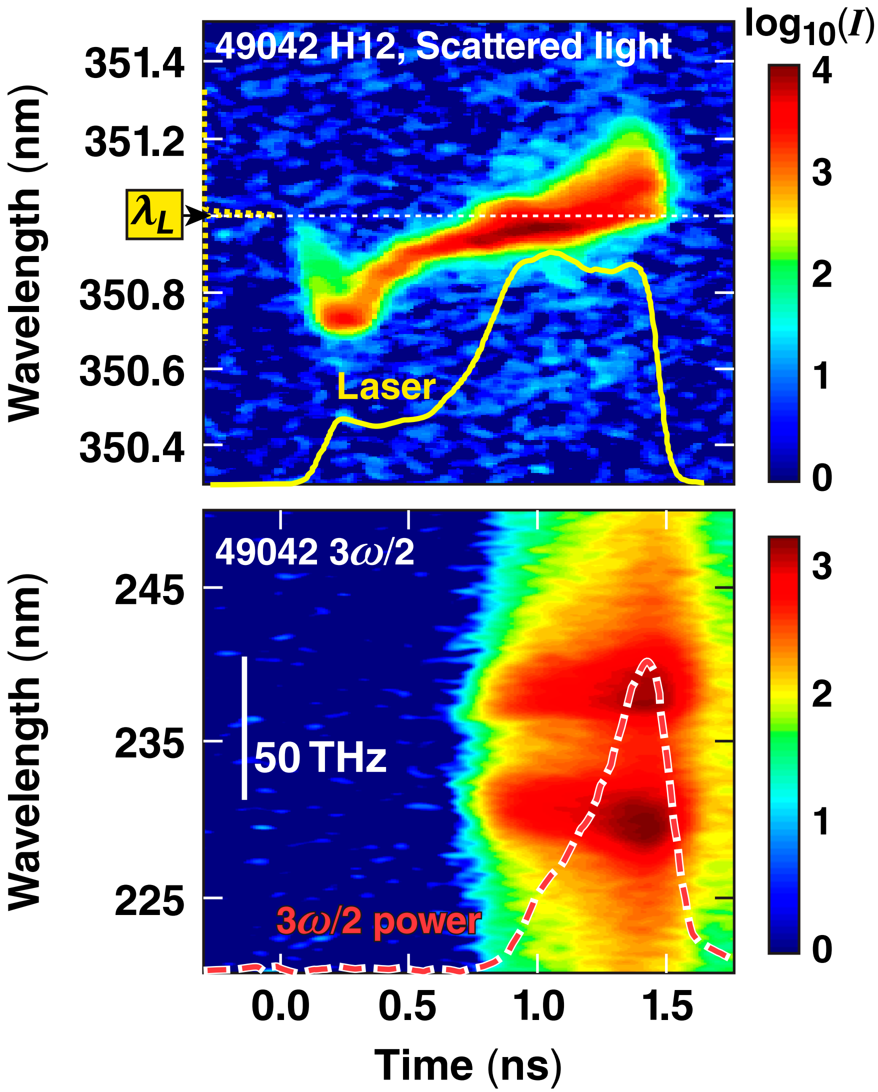

Warm 10 μm Si(6%)CH + 14 μm CD shell, 849-μm diam, 60 beams, No SSD

E16309a

$3\omega/2$ and $\omega/2$ emission are indicative of the two-plasmon-decay instability and concomitant fast-electron generation

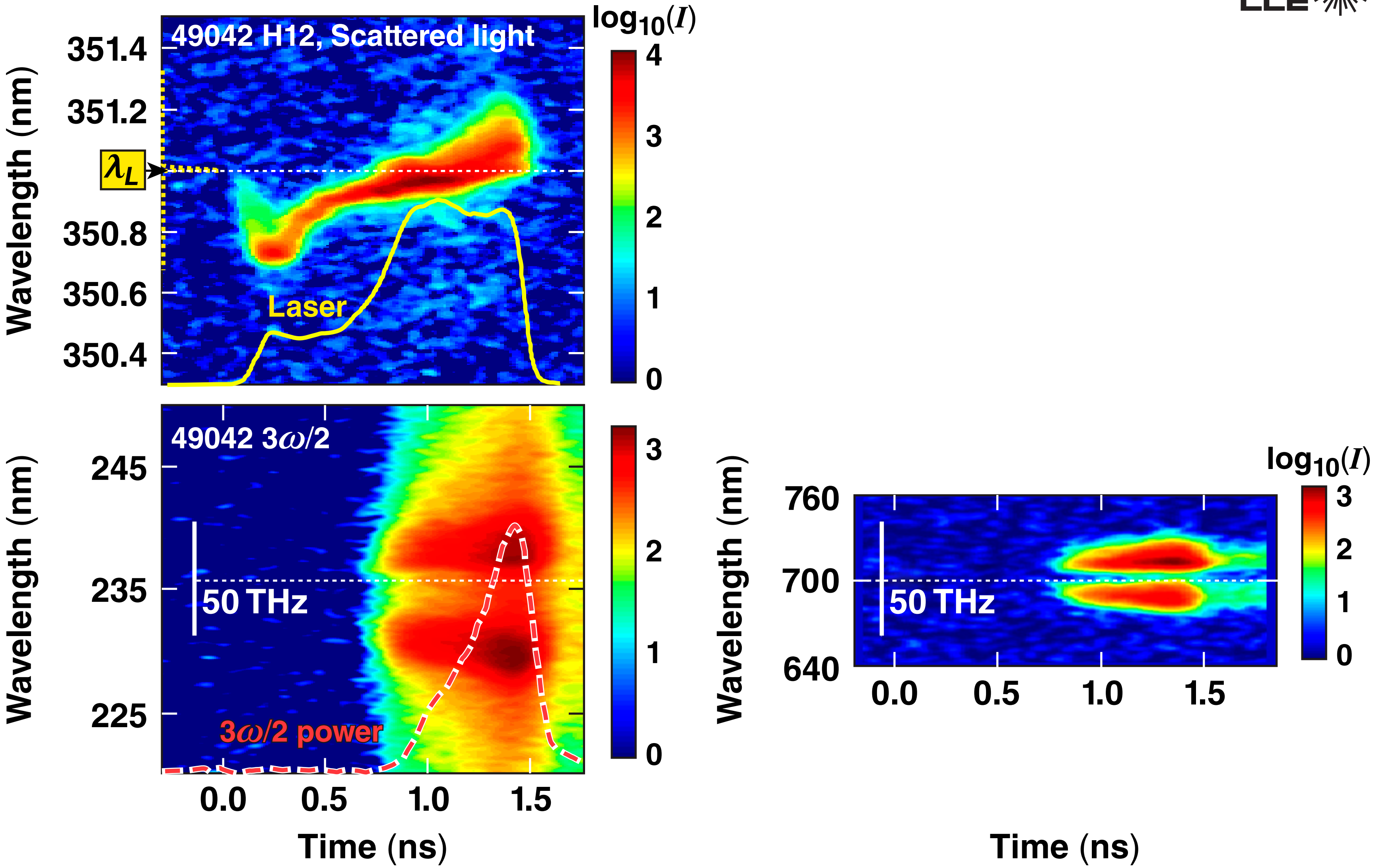

Warm 10 μm Si(6%)CH + 14 μm CD shell, 849-μm diam, 60 beams, No SSD

E16309b

$3\omega/2$ and $\omega/2$ emission are indicative of the two-plasmon-decay instability and concomitant fast-electron generation

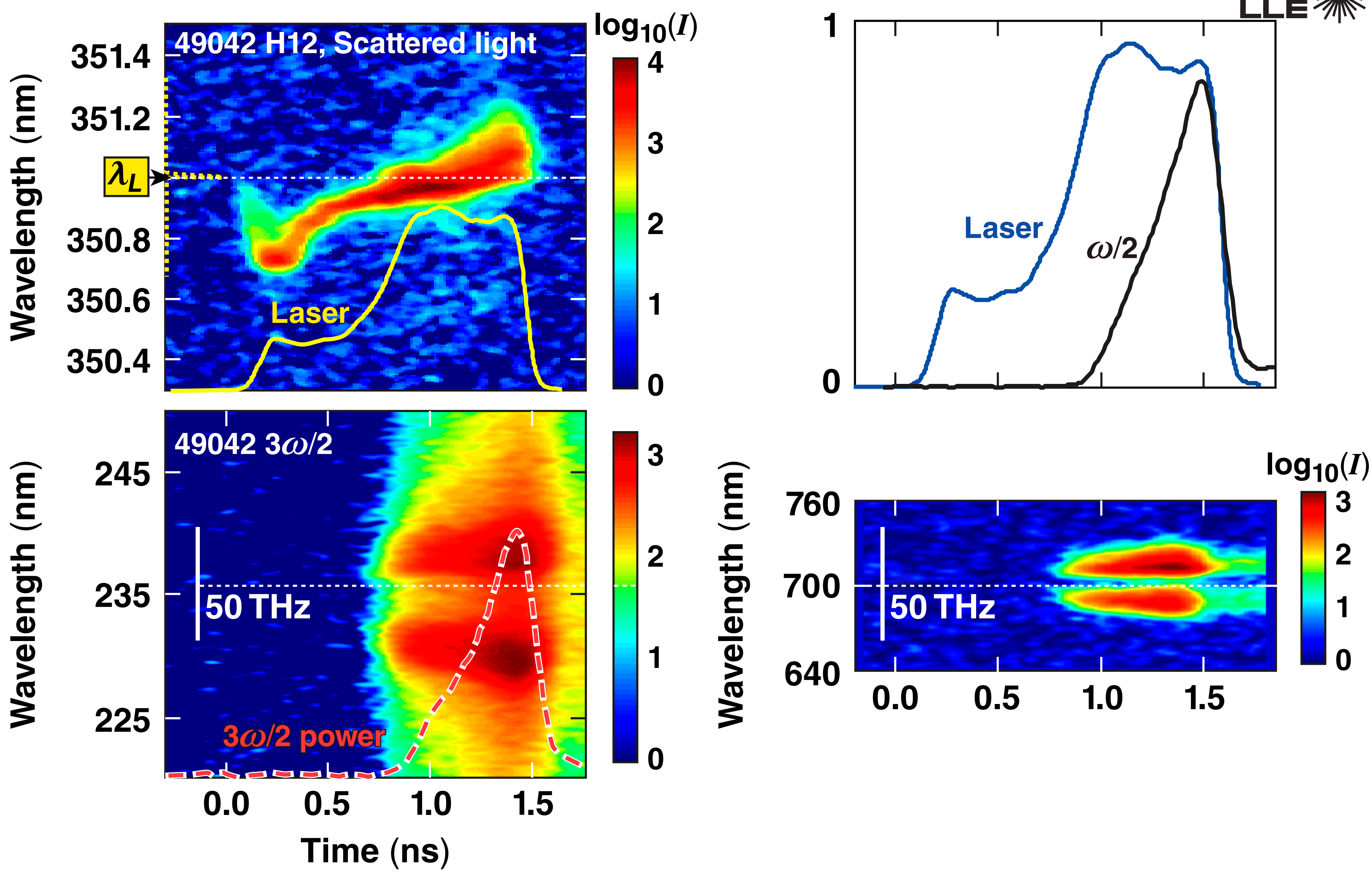

Warm 10 μm Si(6%)CH + 14 μm CD shell, 849-μm diam, 60 beams, No SSD

E16309c

$3\omega/2$ and $\omega/2$ emission are indicative of the two-plasmon-decay instability and concomitant fast-electron generation

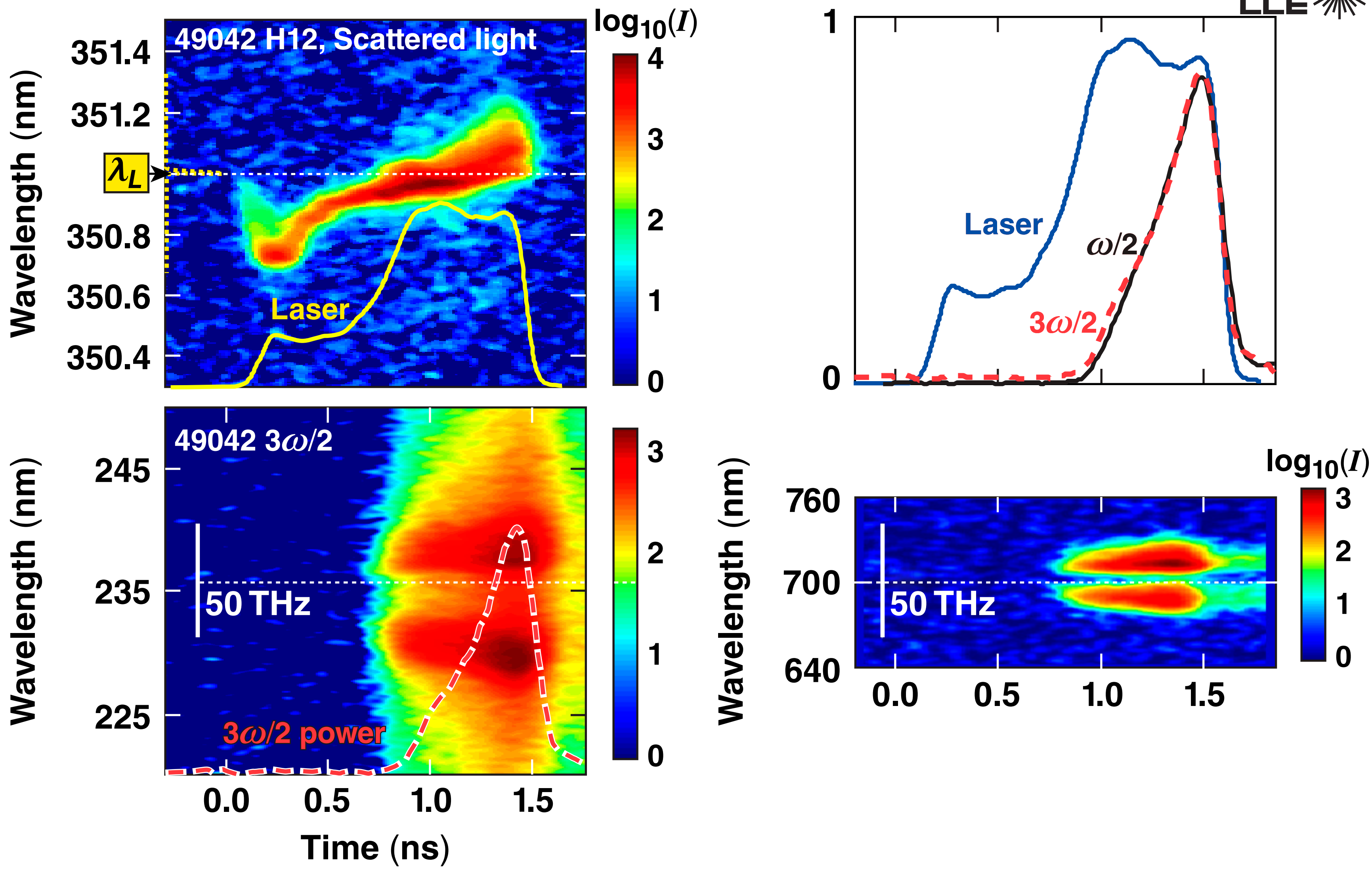

Warm 10 μm Si(6%)CH + 14 μm CD shell, 849-μm diam, 60 beams, No SSD

E16309d

$3\omega/2$ and $\omega/2$ emission are indicative of the two-plasmon-decay instability and concomitant fast-electron generation

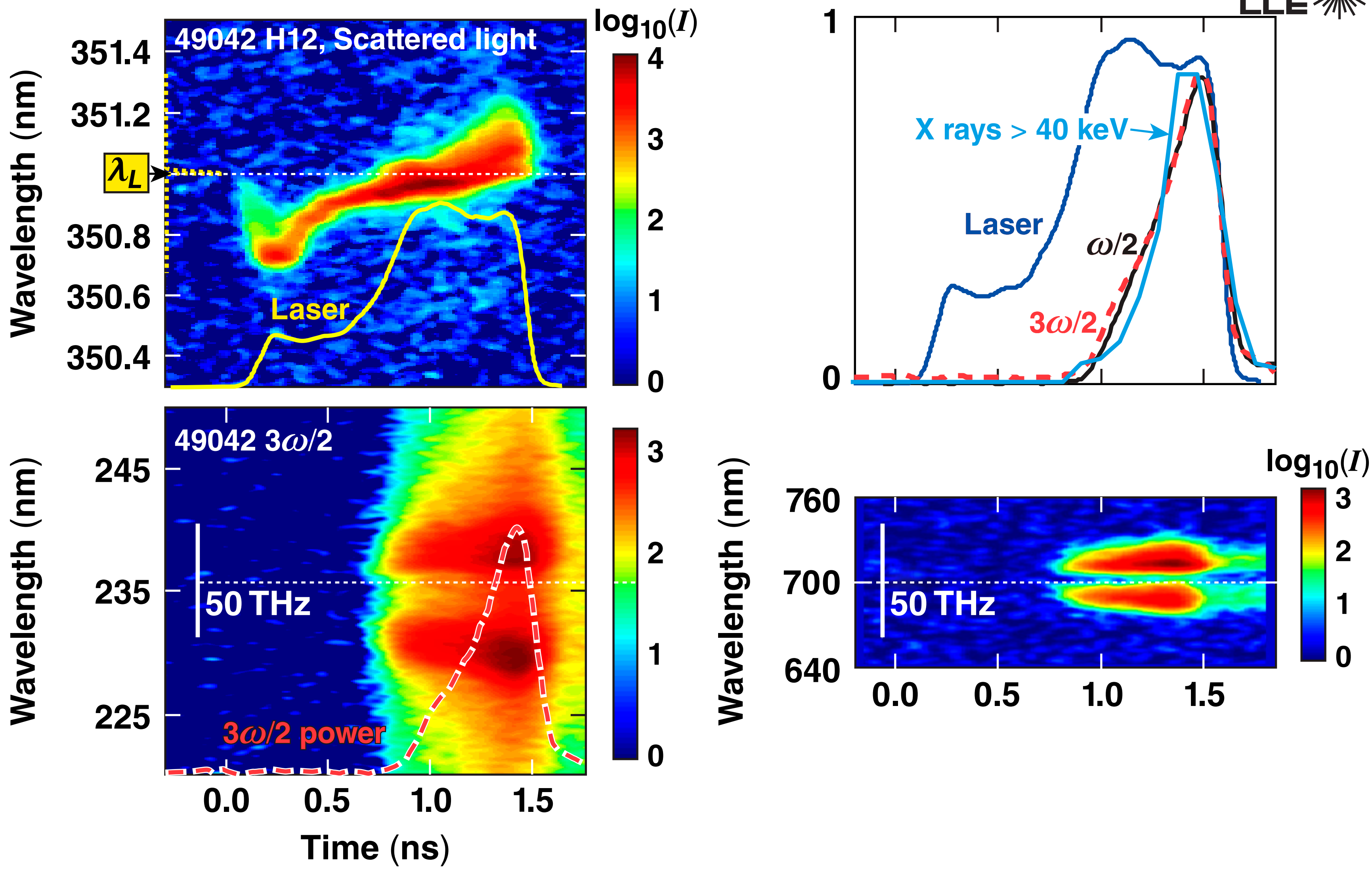

Warm 10 μm Si(6%)CH + 14 μm CD shell, 849-μm diam, 60 beams, No SSD

E16309e

The strong intensity scaling of the hard x rays is clearly evident if pulse shapes and targets remain unchanged

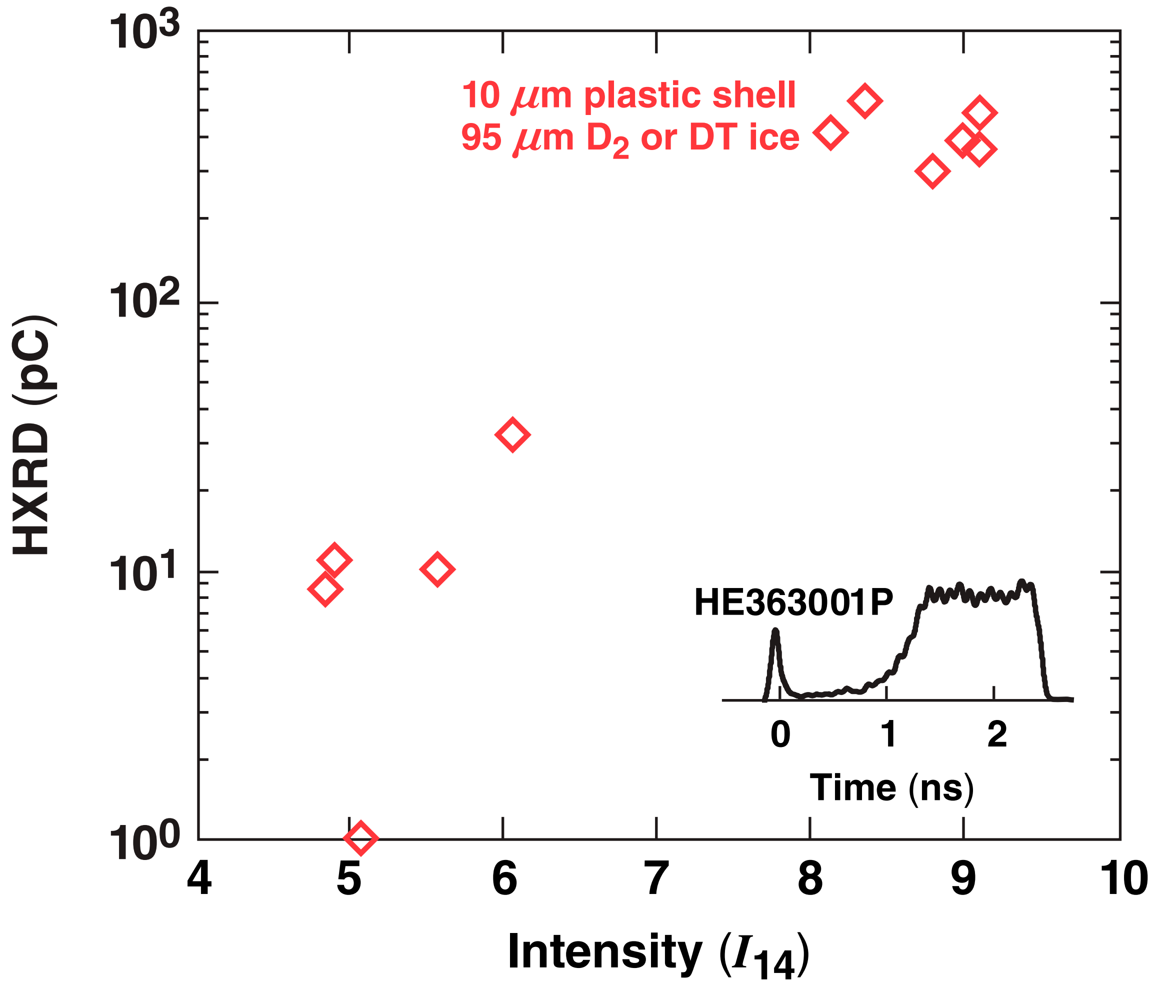

E16310

The strong intensity scaling of the hard x rays is clearly evident if pulse shapes and targets remain unchanged

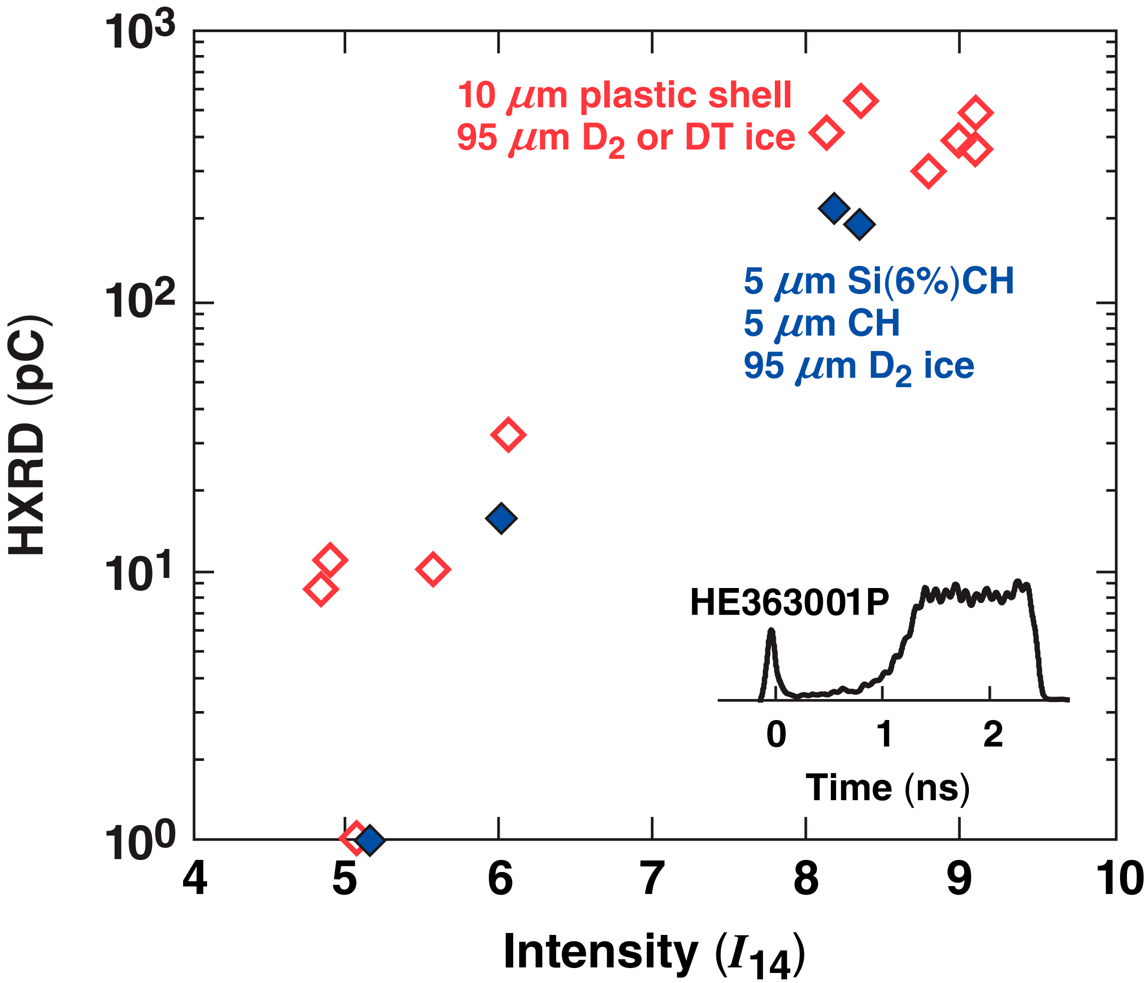

The strong intensity scaling of the hard x rays is clearly evident if pulse shapes and targets remain unchanged

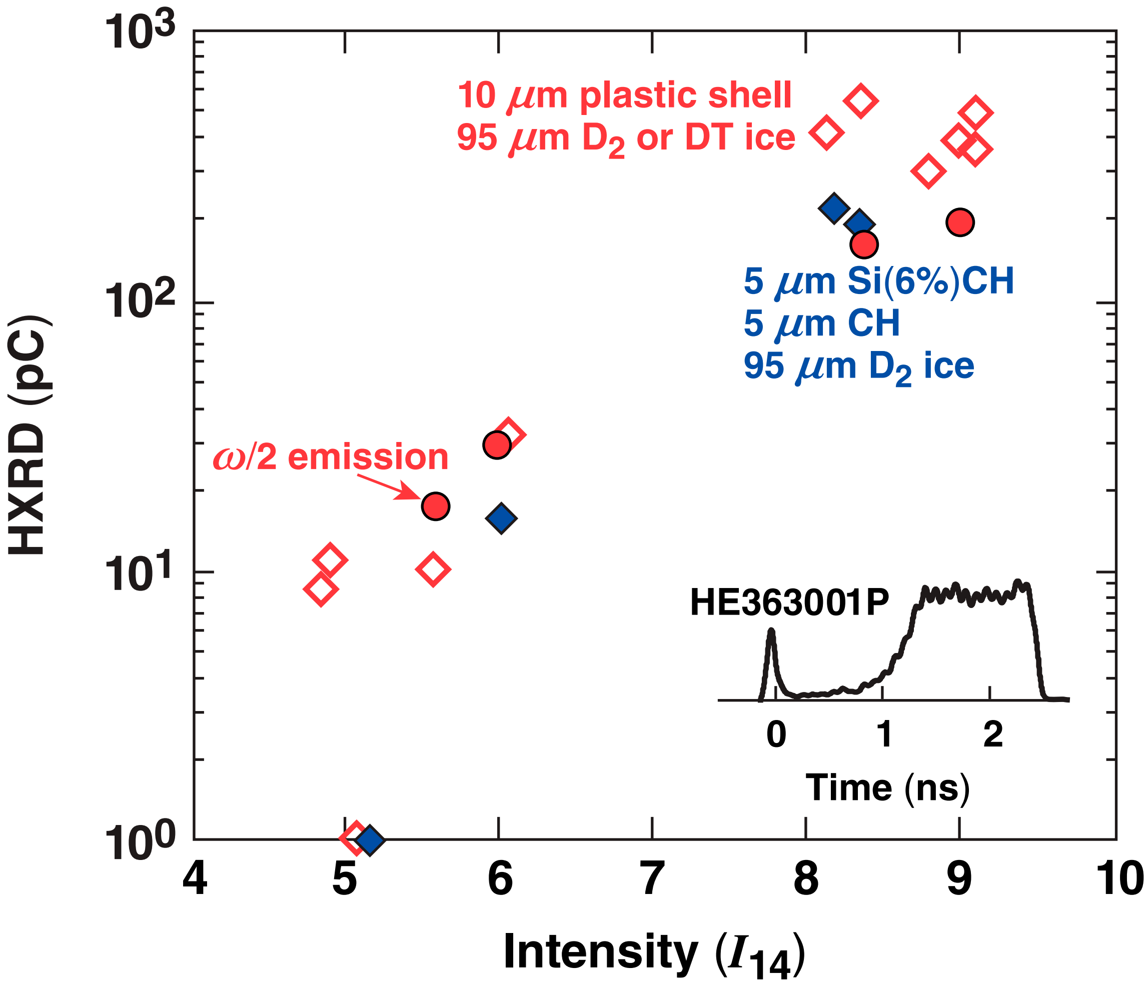

E16310b

The 3/2 harmonic emission depends sensitively on intensity, density scale length, and electron temperature

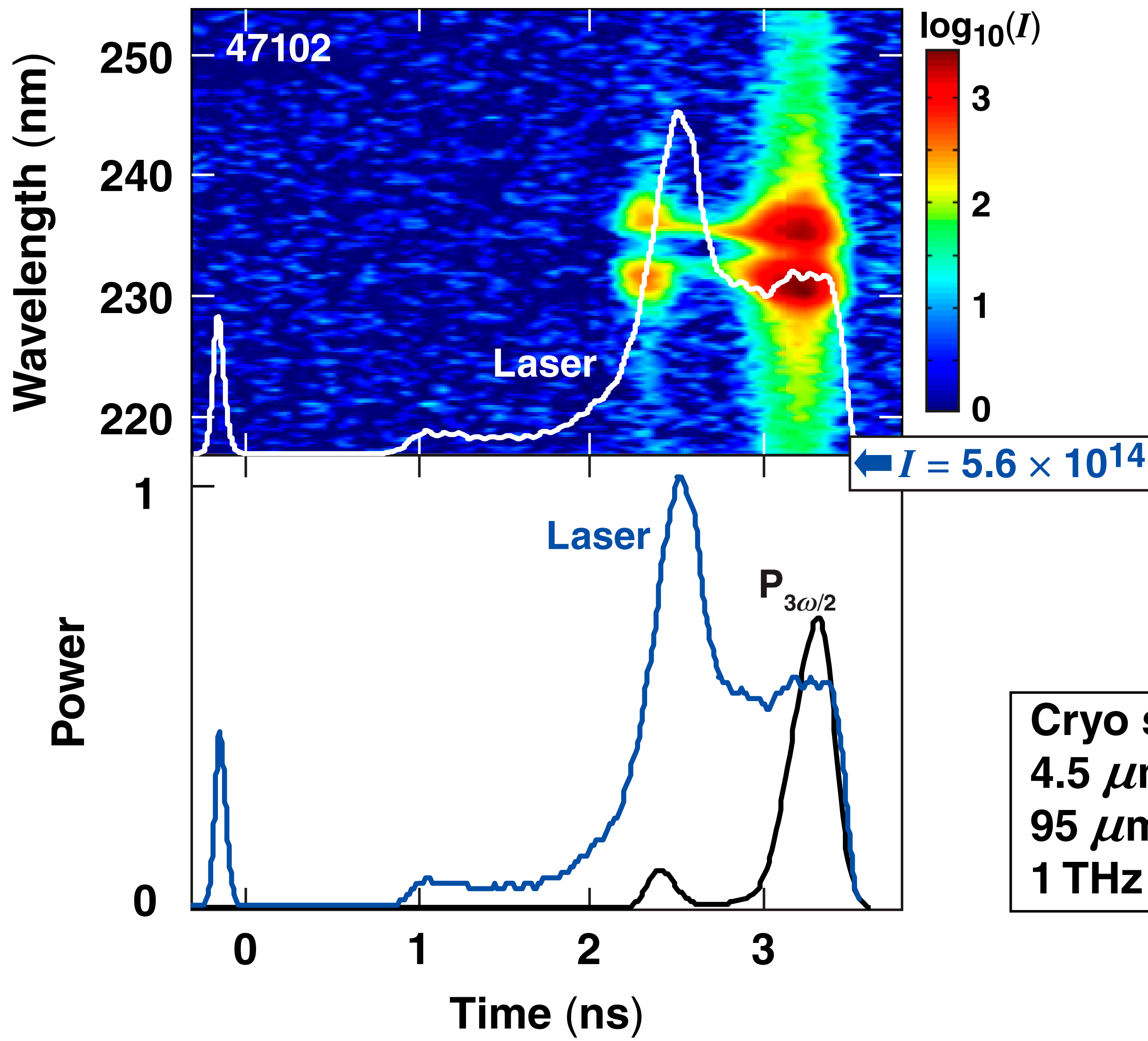

Cryo shot
4.5 μm CH shell
95 μm D_2 ice
1 THz SSD

E16210-4

The 3/2 harmonic emission depends sensitively on intensity, density scale length, and electron temperature

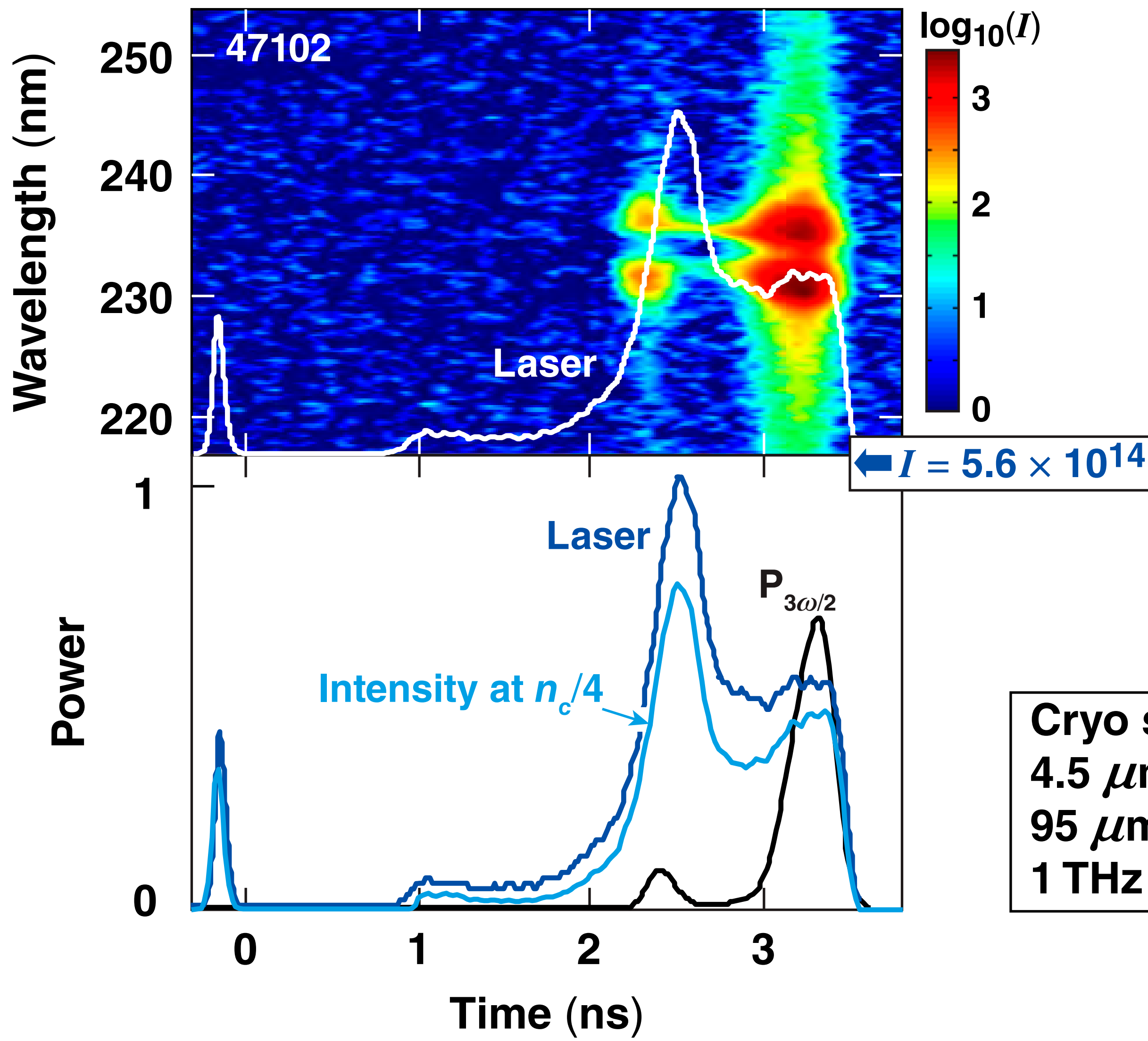

Cryo shot
4.5 μm CH shell
95 μm D_2 ice
1 THz SSD

E16210-2

The 3/2 harmonic emission depends sensitively on intensity, density scale length, and electron temperature

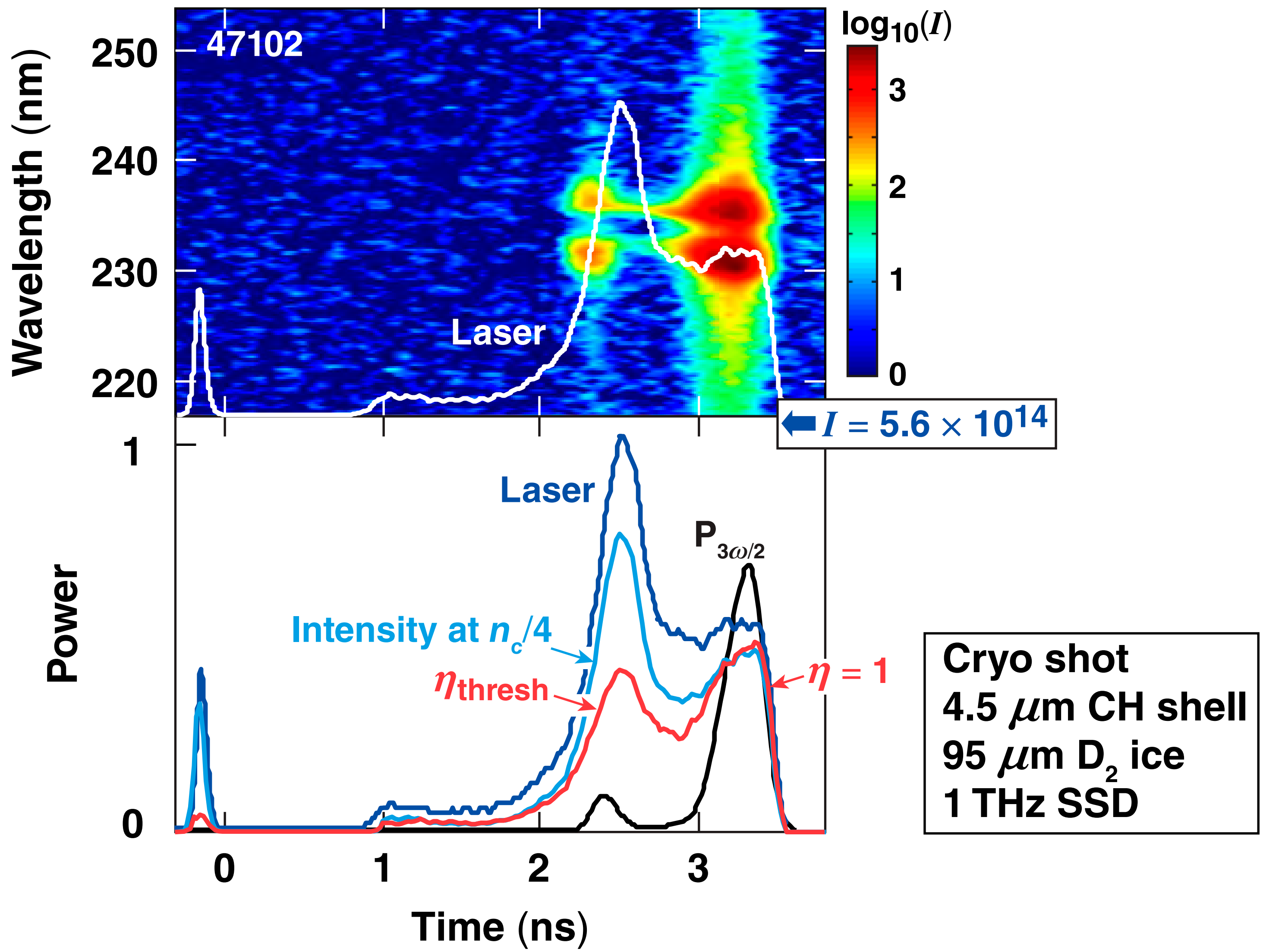

E16210-4

The 3/2 harmonic emission depends sensitively on intensity, density scale length, and electron temperature

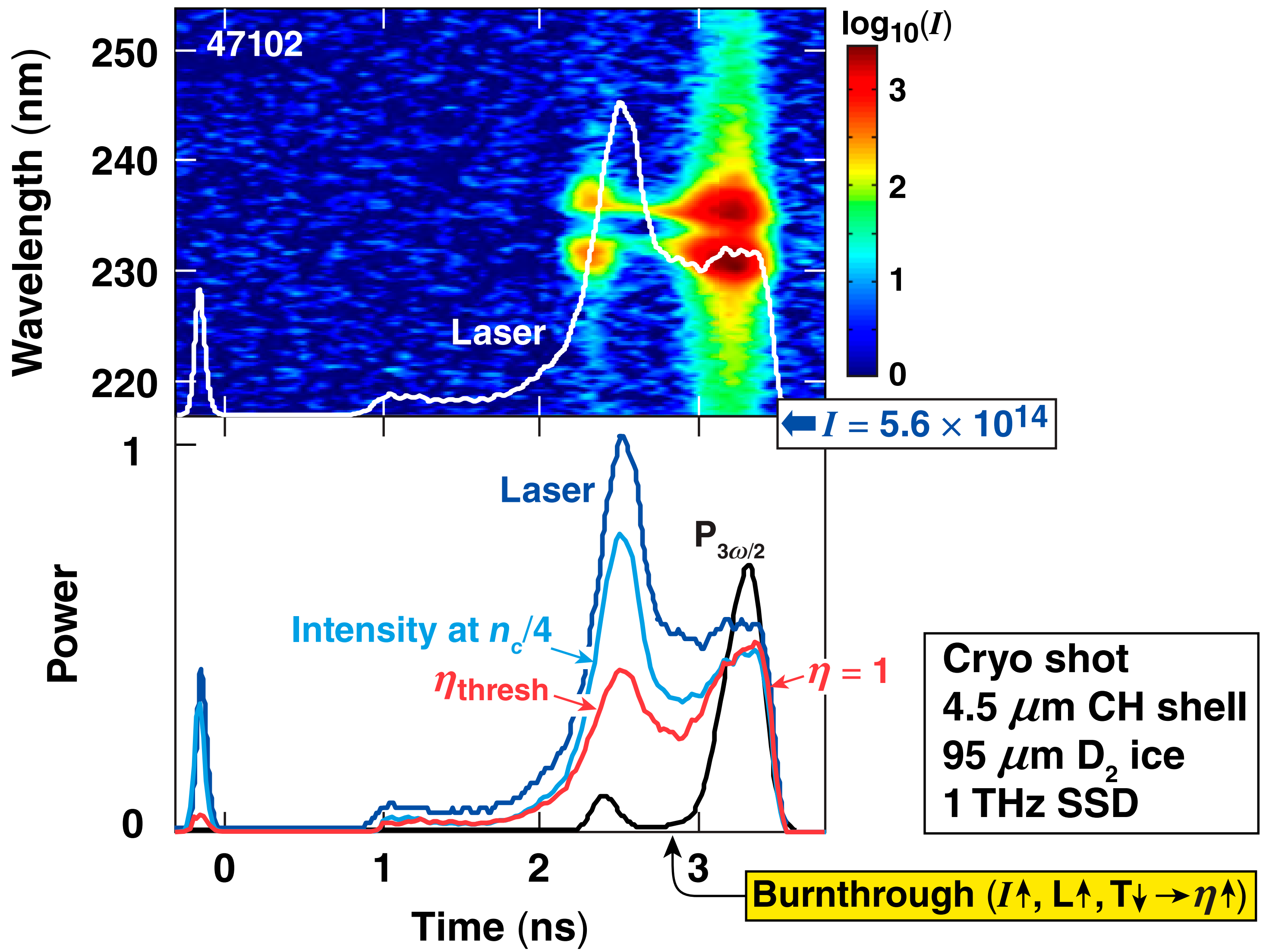

E16210-4

Summary/Conclusions

Time-resolved scattered-light diagnostics provide unprecedented constraints for hydrodynamic simulations

- Time-resolved absorption constrains the electron-heat transport in hydrodynamic simulations.

  nonlocal electron-transport model* in *LILAC*

- The coronal evolution is recorded in the overall scattered-light spectrum and further constrains heat transport.
- Laser–plasma interaction processes are identified through their spectral signatures.
  - enhanced scattering (cross-beam energy transfer)
  - two-plasmon-decay instability
- High-Z doping of plastic shells reduces energetic electron production due to two-plasmon-decay instability.

E16201

*V. N. Goncharov (GI1.00001)